



Semi-equilibrated global sea-level change projections for the next 10,000 years

Jonas Van Breedam¹, Heiko Goelzer^{1*}, Philippe Huybrechts¹

¹ Earth System Science and Departement Geografie, Vrije Universiteit Brussel, Pleinlaan 2, B-1050 Brussel, Belgium

5 * Now at: Institute for Marine and Atmospheric research Utrecht, Utrecht University, The Netherlands

Correspondence to: Jonas Van Breedam (jonas.van.breedam@vub.be)

10

15

20



Abstract. The emphasis for informing policy makers on future sea-level rise has been on projections by the end of the 21st century. However, due to the long lifetime of atmospheric CO₂, the thermal inertia of the climate system and the slow equilibration of the ice sheets, global sea level will continue to rise on a multi-millennial timescale even when anthropogenic CO₂ emissions cease completely during the coming decades to centuries. Here we present global sea-level change projections due to melting of land ice combined with steric sea effects during the next 10,000 years calculated in a fully interactive way with the Earth System Model of Intermediate Complexity LOVECLIMv1.3. The climate forcing is based on the Extended Concentration Pathways defined until 2300 AD with no carbon dioxide emissions thereafter and the inclusion of a methane-emission feedback for the highest forcing scenario, equivalent to a cumulative CO₂ release of around 460 to 5800 GtC. After 10,000 years, the sea-level change rate drops below 0.05 m per century and a semi-equilibrated state is reached. The Greenland ice sheet is found to nearly disappear for all forcing scenarios. The Antarctic ice sheet contributes only about 1.6 m to sea level for the lowest forcing scenario with a limited retreat of the grounding line in West Antarctica. For the higher forcing scenarios, the marine basins of the East Antarctic ice sheet also become ice free, resulting in a sea-level rise of up to 27 m. The global mean sea-level change after 10,000 years ranges from 9.2 m to more than 37 m. The projections of multi-millennial semi-equilibrated sea-level rise for a given CO₂ forcing are shown to be in good agreement with geological archives.

1 Introduction

Modern sea-level rise started at the end of the 1800s and has accelerated over the course of the 20th century (Church and White, 2011, Hay et al., 2015) with an unprecedented rate over the observational era during the first part of the 21st century (Watson et al., 2015). The rate of sea-level rise was 2.5 times larger during the last decade than during most of the 20th century (Oppenheimer et al., 2019). So far, the horizon for most global mean sea-level change projections has been the end of the 21st century (Jackson and Jevrejeva, 2016, Kopp et al., 2017, Goelzer et al., 2020b, Seroussi et al., 2020). Sea-level change projections beyond 2300 are scarce (Clark et al., 2016). However, due to the long lifetime of carbon dioxide in the atmosphere (Archer et al., 2009b) and the thermal inertia of the climate system (Solomon et al., 2009, Gillett et al., 2011, Goelzer et al., 2012), sea level is expected to continue to rise on a multi-centennial to multi-millennial timescale. Moreover, the large ice sheets themselves have a very long response time to any perturbations (Golledge, 2020) with the longest response time ranging from 10,000 years for accumulation rate changes to up to 100,000 years for temperature changes for the Antarctic ice sheet (Alley and Whillans, 1984).

On a multi-millennial timescale, changes in land ice volume (mass contribution) together with ocean density changes from thermal expansion (thermosteric contribution) and haline contraction (halosteric contribution) are the main components contributing to global sea-level change (Miller et al., 2005). The mass contribution comes from melting or growing of the Antarctic ice sheet, the Greenland ice sheet and glaciers and ice caps. The steric contribution is the expansion of ocean water



when it gets warmer and less saline or conversely, the contraction when water is cooling and gets more salty (Feistel, 2010). The magnitude of thermal expansion depends on the climatic temperature forcing and on the rate of oceanic heat uptake. Because of the large mass and slow turnover time of the deep ocean, the oceanic heat content (and hence thermal expansion) will continue to rise in the ocean for centuries to millennia, even when surface warming has halted. Haline contraction – or expansion of ocean water due to freshening – is a smaller, though not negligible component of steric sea-level rise. Physically-based models have been used to study the different components contributing to global sea level on a multi-millennial timescale. For example, long-term ice sheet evolution and resulting sea-level change projections have been made for the next few millennia for the Greenland ice sheet (Charbit et al., 2008, Robinson et al., 2012, Applegate et al., 2015), the Antarctic ice sheet (Huybrechts, 1993, Golledge et al., 2015, Pollard et al., 2015, Winkelmann et al., 2015, DeConto and Pollard, 2016) or both (Vizcaino et al., 2008, Huybrechts et al., 2011).

Existing long term sea-level change projections including both the changes in land ice volume and the steric components extend for the next 2000 years (Levermann et al., 2013) or 10,000 years (Clark et al., 2016). These studies did not take the full coupling between the ocean and the atmosphere into account, which becomes important when the ice sheets lose large volumes of freshwater. Goelzer et al. (2012) studied the committed sea level rise at the end of 3000 AD with a coupled model approach for a range of idealised CO₂ scenarios. So far, the study of semi-equilibrated sea level changes including all components of future sea-level change with the incorporation of feedbacks between the climate components has not been performed because of the high computational cost. The adopted trade-off between model complexity and model interactions on a multi-millennial timescale consists of the use of the Earth System Model of Intermediate Complexity LOVECLIM with a lower resolution but fully integrated coupling.

In this study, we project the global mean sea level changes for the next 10,000 years in a fully interactive way between all major components in the climate system. The duration of the simulations allows the climate system to reach a semi-equilibrated state, long time after the cessation of anthropogenic greenhouse gas emissions. The greenhouse gas forcing follows the Extended Concentration Pathway (ECP) scenarios to span the likely range in climate uncertainty with the inclusion of a methane-emission feedback in a warming climate.

2 Model description and initialisation

High resolution general circulation models (GCM) are the best tools to project climate changes until the end of the century or a few hundred years after that, but they are computationally too expensive to make millennial to multi-millennial projections. Earth System Models of Intermediate Complexity (EMIC) have a lower resolution and therefore allow for longer simulations such as simulating the climate over the last millennium (Eby et al., 2013) or exploring climate-carbon cycle feedbacks during the next 1000 years (Zickfeld et al., 2013). Here we make use of the EMIC LOVECLIMv1.3 (Goosse et al., 2010) for the projections of global sea-level change on a multi-millennial timescale. LOVECLIM is one of the few EMICs with an ice sheet



component (AGISM) that is fully coupled to the other components of the climate system (ECBilt for the atmosphere – CLIO for the ocean and sea-ice – VECODE for the terrestrial biosphere), allowing for multi-millennial projections of sea-level change. ECBilt is a quasi-geostrophic atmospheric model with truncation T21, corresponding to a resolution in longitude and latitude of approximately 5.625° and three vertical levels (Opsteegh et al., 1998). CLIO is a global free surface ocean GCM coupled to a thermodynamic sea-ice model, with a resolution of 3° in longitude and latitude and 20 unevenly spaced vertical levels (Goosse and Fichefet, 1999). AGISM, the ice sheet model component consists of 3-D thermomechanically coupled ice sheet models for the Greenland ice sheet and the Antarctic ice sheet (Huybrechts and de Wolde, 1999) and is run at a resolution of 10 km for the Greenland ice sheet and 20 km for the Antarctic ice sheet. The relative coarse resolution is necessary to allow for long integrations (10,000 model years take 20+ days of computational time). The global glacier melt algorithm is based on the model of Raper and Braithwaite (2006) that considers a total sea-level equivalent (SLE) of 0.241 m (mountain glaciers contain 41% of this estimate while the ice caps are responsible for the other 59% of SLR potential). This is at the lower end of the range of total recent estimates of ice volume (0.24 – 0.40 m SLE) stored in all ~215 000 glaciers on Earth (Farinotti et al., 2019), partly explained by the fact that the glacier model excludes glaciers in the periphery of the Greenland and Antarctic ice sheet. The steric sea level change component, thermal expansion and haline contraction, is calculated based on regional changes in ocean temperature and salinity. The ocean carbon cycle is not activated and greenhouse gas concentrations are prescribed (see Sect 3. and Appendix A).

The model has been used previously for ice sheet and climate change projections for periods in the past (Loutre et al., 2014, Goelzer et al. 2016a, 2016b) and the future (Huybrechts et al., 2011, Goelzer et al., 2012). The version used here differs from LOVECLIMv1.3 for the Antarctic ice sheet component by including surface ablation on the ice shelves, an important process under future atmospheric warming. A tundra warming feedback is also included for retreating ice sheets by making a distinction between snow/ice albedo and tundra albedo. The snow/ice albedo is replaced by tundra albedo (with a lower albedo) once the ice sheet margin is retreating on land. In order to better represent the climate forcing for the ice sheet models, temperature and precipitation anomalies are applied to eliminate the bias from a coarse resolution atmospheric model. The surface mass balance is calculated using the PDD method for both ice sheet models. The Antarctic ice sheet model uses the shallow ice approximation (SIA) for grounded ice and the shallow shelf approximation (SSA) for the ice shelves coupled across a one grid cell wide transition zone. Basal melting is calculated as a function of the mean oceanic heat input into the ice shelf cavities. Sea-level changes resulting from melting of the marine-based parts of the Antarctic ice sheet are corrected for bedrock elevation changes (Goelzer et al., 2020a). Both ice sheet models have recently participated in the ISMIP6 initiative (Goelzer et al., 2020b; Seroussi et al., 2020).

Since many physical parameters in a climate model are uncertain, LOVECLIM is used to explore the climate response for a large combination of climate model parameter sets (Loutre et al., 2011). Here we have evaluated 4 different model parameter sets by testing the sea-level contribution for the period 1900-2300 AD. The 4 model parameter sets (P11, P22, P32a, P32b; see Table S3) differ in their sensitivity to the applied greenhouse forcing ($P32b > P32a > P22 > P11$) and freshwater forcing in the



120 North Atlantic (P32a, P32b and P22 > P11). All climate model parameter sets yield climate simulations in agreement with observations over the past 500 years (Loutre et al., 2011). Model parameter set P22 is chosen for the multi-millennial integrations because of its mid-range contribution to sea-level at 2100 AD and 2300 AD in comparison with recent studies (Pörtner et al., 2019; Calov et al., 2018; Bulthuis et al., 2019; Tables S1-S2 and Figure S1). The mean annual temperature anomalies over the ice sheets for 2070-2100 relative to 1970-2005 (+4.6°C over Greenland and +3.8 °C over Antarctica for RCP8.5) correspond well with the mid to upper ranges of AOGCM projections over the polar regions (Fettweis et al., 2013, Barthel et al., 2019). With an equilibrium climate sensitivity of 2.3°C, the model parameter set is at the lower end of IPCC AR5 estimates (likely range of 1.5°C - 4.5°C) due to a cold bias in the tropics.

125 The Greenland ice sheet and Antarctic ice sheet are spun-up from standalone experiments forced with reconstructed temperature forcing above the ice sheet following ice core records for respectively two and four glacial-interglacial cycles to carry their long-term ice sheet history (Huybrechts et al., 2011; Goelzer et al., 2012). A quasi-equilibrium experiment is run with the aim to get a climate in equilibrium at 1500 AD with the ice sheet forcing. The ice sheet models in this experiment evolve very slowly without seeing the changes of the climate model. The climate model on the other hand is subject to changes in the ice sheet models (changes in freshwater flux, albedo and height changes) and equilibrates to these boundary conditions.

130 At the end of the quasi-equilibrium run (after 2500 years), a steady state is reached. A control experiment with constant pre-industrial greenhouse gas forcing showed that the drift in climate and ice sheet components is negligible. The climate information present at the end of the quasi-equilibrium experiment is used as input for the initialisation of the fully coupled experiments starting at 1500 AD.

135 The fully coupled model is run from 1500 to 2000 AD. LOVECLIM is forced during this historical period with known greenhouse gas concentrations, total solar irradiance and volcanic forcing. Now, all components of LOVECLIM interact dynamically and are run as an ensemble of five members. The ensemble members are identical except for small perturbations in the initial conditions. Five iterations of the reference state for the ice sheet models are performed to see if there is convergence for the climatic information (e.g. Greenland and Antarctic temperature forcing, oceanic heat content and meridional overturning circulation variability).

140 The experiment performing best at representing the climate over the last 500 years is chosen as input for the long-term future projections.

3 Scenario description

Six different forcing scenarios are constructed to span a large range of future greenhouse gas forcing. The main difference between the different scenarios is the atmospheric carbon dioxide forcing. Four of the CO₂ forcing scenarios are extensions of the ECP scenarios (Meinshausen et al., 2011) and will be referred to as Multi-Millennial Concentration Pathways (MMCPs) with the same designation as the RCP scenarios (MMCP2.6, MMCP4.5, MMCP6.0 and MMCP8.5). The scenarios range from a peak in the CO₂ concentration of 443 ppmv in 2053 AD with temporarily negative emissions thereafter (MMCP2.6) to a



150 peak of 1962 ppmv in 2250 AD (MMCP8.5). Total recoverable carbon (oil, gas, lignite and coal) reserves (the total exploitable
carbon) and resources (total carbon mass stored on earth, including the non-exploitable carbon) estimates are disputed, ranging
155 from < 1500 GtC reserves and 4000 GtC resources (Hasselmann et al., 2003) up to 2900 GtC reserves and 11000 GtC resources
(McGlade and Ekins, 2015). In this study, the MMCP scenarios (extended ECP scenarios with zero emissions after 2300 AD)
are equivalent to a total cumulative emission ranging from less than 200 GtC for scenario MMCP2.6 to more than 5000 GtC
for scenario MMCP8.5 relative to the year 2000 AD (see Appendix: Table A3). This is comparable to the study from Clark et
al. (2016) with an emission pulse of 1280-5120 GtC, but well below the study from Winkelmann et al. (2015) that assumes a
total carbon release of up to 10,000 GtC.

Two additional scenarios are constructed. The first one assumes that CO₂ concentrations follow ECP8.5 but emissions will
cease completely by the year 2150 AD. This scenario is referred to as MMCP-break and is an intermediate forcing scenario
between MMCP6.0 and MMCP 8.5. The second additional scenario (MMCP-feedback) assumes that methane emissions
increase as a feedback to the warming climate (Table A3). The size of the methane reservoir is a major unknown and estimates
160 range from 500-3000 GtC (Piñero et al., 2013) to 5000-20,000 GtC (Dickens, 2011). Ruppel and Kessler (2017) made an
extensive review to estimate the size of the methane hydrate reservoir and finds a converging value of around 2000 GtC.
MMCP-feedback assumes a moderate methane release from methane hydrates of 600 GtC by adding constantly CO₂ after 2250
AD (from the peak concentration onwards) until the end of the simulations, in accordance with the experiments of Archer et
al (2009a). At least 50% of the methane released from the hydrates would be anaerobically oxidised inside the seafloor and an
165 additional part is converted into CO₂ in the water column by aerobic oxidation (Treude et al., 2003). In our experiments, it is
assumed that the methane released from methane hydrates is completely oxidised in CO₂ when it reaches the atmosphere.

The carbon dioxide concentrations follow the ECP scenarios until 2300 AD with zero emissions thereafter. Impulse response
functions are used to construct the falloff of carbon dioxide concentrations (Appendix A). Carbon cycle models show that a
perturbation of CO₂ can remain for tens of thousand of years in the atmosphere (Archer et al., 2009b, Lord et al., 2016). After
170 a perturbation, atmospheric carbon is taken up by the land biosphere (~100 years), ocean invasion (10-1000 years), CaCO₃
weathering (1000-10,000 years) and silicate weathering (10,000-1,000,000 years) to eventually restore the initial
concentrations (Ciais et al., 2013). The more carbon is emitted, the slower the uptake of carbon dioxide in the ocean due to the
reduction in buffering capacity (Archer et al., 2009b). The constructed carbon dioxide concentrations for the next 10,000 years
take these effects into account in a schematic way and are shown in Figure 1a.

175 Methane (average lifetime of 9 years) and nitrous oxide (average lifetime of 131 years) concentrations are kept constant at
their concentration in 2300 AD (Meinshausen et al., 2011) because of the high rates of natural emissions and the increase in
natural emissions for a warming climate. The increase in natural emission of methane are ascribed to the increase in natural
wetland methane emissions in a warmer climate (Kirschke et al., 2013). Higher decomposition rates in a warming climate are
responsible for an increase in nitrous oxide emissions (Griffis et al., 2017). Other greenhouse gases (methane and nitrous



180 oxide) follow the trajectory until 2300 AD as presented in Meinshausen et al. (2011) and either decrease to zero when the trend is declining and the lifetime of the gases is short (chlorofluorocarbons, CCl_4 and CH_2CCl_3) or stay constant over the next 10,000 years when the overall trend is unclear (hydrofluorocarbons and hydrochlorofluorocarbons).

The orbital parameter variations are included in the climate forcing. However, the insolation differences in the polar regions are rather small (summer insolation will slightly increase in the northern hemisphere and decrease in the southern hemisphere compared to the present-day) on account of a low eccentricity and therefore its influence on the radiative forcing is limited. 185 The future solar forcing is unknown and therefore the last 11-year solar cycle is repeated for the next 10,000 years.

4 Climate response and global sea-level budget of individual terms

In the following sections, the climate response to the greenhouse gas forcing and insolation variations and the sea-level changes resulting from mass changes of the Greenland ice sheet (GrIS), the Antarctic ice sheet (AIS) and glaciers and ice caps, and thermal expansion and haline contraction of the ocean water are shown. The relative importance of each contribution to global 190 mean sea level (GMSL) following a specific scenario is discussed.

4.1 Climate response

Global mean surface air temperature (SAT) is projected to increase between 1.7°C and 5°C following the strong increase in greenhouse gas forcing (Figure 1). In the polar regions, the reduction in sea ice area and its large effect on absorption of heat through the ocean surface albedo leads to an amplified response to the climatic forcing. Moreover, the height-mass balance 195 feedback and the albedo-temperature feedback causes the GrIS mean annual SAT to rise even further as ice is melting. This is most obvious for the mean annual SAT anomaly using scenarios MMCP2.6 to MMCP-break where the SAT is increasing strongly when the GrIS melted an equivalent of around 2 m sea level (Figure 1c). The increase in Antarctic mean temperature over the next 10,000 years shows a very large spread between the different scenarios. This is partly caused by a decreasing 200 sea-ice area trend and its influence on the albedo, where the retreat will be larger for the high forcing scenarios (Figure 9). Snow accumulation is projected to increase for all forcing scenarios due to the increase in atmospheric water vapor, whereas the increase in accumulation will be larger for the strongest warming scenarios (up to 16 % for scenario MMCP-feedback over the Antarctic continent). Freshwater fluxes from the Greenland and Antarctic ice sheets lead to temporarily reduced temperatures and a delayed peak warming over the ice sheets.

205 4.2 Thermal expansion and haline contraction

The projections for thermal expansion and haline contraction show an increase following global mean temperature perturbations with the longer response time for the higher forcing scenarios. Thermal expansion and haline contraction rise rapidly before showing a period of stabilization for all scenarios. Except for scenario MMCP2.6 and MMCP4.5, this period is



210 followed by another more gradual increase in sea-level rise during the second half of the simulations (Figure 4). This is most
pronounced for scenario MMCP6.0 and MMCP-break where the steric contribution to GMSL rise reaches respectively 0.3 and
0.4 m between 7000 AD and 12,000 AD. Oceanic temperatures have already equilibrated to the forcing and at 12,000 AD,
215 deep ocean temperatures are slightly lower than temperatures at 7000 AD, following the slow decrease in global mean
temperature anomalies (Figure 11). Therefore, we attribute the sea-level rise during the second half of the simulations to the
continued freshwater release from the Antarctic ice sheet. On the other hand, the steric contribution to GMSL slightly decreases
215 for scenarios MMCP2.6 and MMCP4.5 after a peak at 3000 AD. Freshwater fluxes are still high due to a slow melting of the
GrIS, suggesting that the lower increase in global mean temperatures decreases the response time. At the end of the simulations,
the total range of the steric component to GMSL change is between 0.4 m (MMCP2.6) and 3 m (MMCP-feedback) .

4.3 The Greenland ice sheet

220 The GrIS volume changes because of an imbalance between the surface mass balance (SMB), the difference between
accumulation and ablation, and iceberg calving at the ice sheet margin. Surface runoff is projected to increase for any of the
forcing scenarios, though the magnitude differs significantly. After 4000 years, surface runoff exceeds accumulation and the
surface mass balance becomes negative even for the lowest forcing scenario (Figure 2c). In a high warming scenario, this
might happen already at the end of the 21st century (Figure 2d). When looking at all the mass balance components, one can see
225 that the relative importance of iceberg calving decreases when the ice sheet retreats on land. The large amounts of meltwater
result in a total freshwater flux anomaly of 0.03 to 0.05 Sv for the three higher forcing scenarios and is sustained for 1000 to
1500 years (Figure 7a). The Atlantic Meridional Overturning Circulation (AMOC) almost completely shuts down for the two
highest forcing scenarios (Figure 8). This results in a local cooling south of the GrIS and a delayed peak warming above the
Greenland ice sheet (most pronounced for MMCP-feedback; Figure 1c), pointing to the importance of simulations with a
coupled ocean-atmosphere-ice sheet model. The AMOC recovers again after the ice sheet has melted entirely and even
230 becomes stronger for the higher forcing scenarios (Figure 10).

4.4 The Antarctic ice sheet

235 The Antarctic continent is very cold and there is almost no surface melt over the grounded ice at present. There is a very
distinct response of the AIS to a low or a high forcing in terms of mass loss. Looking at the two extremes, ice discharge at the
grounding line is projected to increase slightly for scenario MMCP2.6, similar to previous suggestions that increased ice
discharge is a response to increased accumulation (Winkelmann et al., 2012). The ice shelves thin for 1700 years because of
atmospheric warming, while basal melting rates below the ice shelves remain low with a mean value of 0.3 m per year over
all the ice shelves. The ice shelves lose 2/3 of their volume, but they recover again to reach their initial volume after 5000
years when surface ablation becomes negligible. In scenario MMCP-feedback, even the large ice shelves around Antarctica
disappear nearly completely after 300 years as a combination of atmospheric warming (and subsequent surface ablation) and



240 a quadrupling in ice shelf basal melt rates. Ice discharge across the grounding line is projected to increase for about 500 years
and drops below present-day values after 1700 years when the West Antarctic ice sheet has collapsed and the East Antarctic
ice sheet starts to retreat land inwards. The increase in surface runoff is even stronger and exceeds accumulation at the end of
the first millennium for about 3000 years, after which surface runoff and ice discharge along the grounding line stabilize and
account each for about half of the mass loss (Figure 3d). The freshwater input in the Southern Ocean increases with 0.14 Sv
245 for the highest forcing scenario and remains elevated until the end of the simulations with an anomaly of 0.07 Sv due to
continued ice sheet melting and increased runoff over land (Figure 7b). As a consequence of the freshwater release into the
Southern Ocean, the strength of Antarctic Bottom Water (AABW) declines with 23 % for MMCP2.6 and up to 77 % for
MMCP-feedback during the next 500 years due to rapid ice sheet melting (Figure 8). These freshwater fluxes from the AIS
lead to reduced oceanic warming in the vicinity of Antarctica and relatively low basal melt rates in our experiments (mean
250 basal melt rates of 0.5-1.1 m per year for scenario MMCP-feedback during the coming centuries). Mean SAT anomalies above
the Antarctic ice sheet reach a maximum between 5000 and 6000 AD when the ice sheet retreats on land and the albedo-
temperature feedback sets in (Figure 1d). The mass balance components stabilize during the second half of the simulations
with iceberg calving and ablation both accounting for half of the mass loss, a situation comparable to the Greenland ice sheet
today.

255 There is a very large difference in ice sheet geometry of the AIS after 10,000 years for the lowest and highest forcing scenario.
In scenario MMCP2.6, the grounding line retreats mostly in the Weddell Sea and the Ross Sea basin, with almost no retreat
for the East Antarctic ice sheet (Figure 3a). For the high emission pathway, the West Antarctic ice sheet collapses and
grounding line retreat initiates in the Wilkes subglacial basin (Figure 3b). Due to isostatic rebound of the Earth's crust, more
260 land is exposed above sea-level at 12,000 AD compared to the situation at 7000 AD and the ice sheet margin becomes land-
based for most of East Antarctica as has been proposed for warm intervals during the mid-Miocene (Gasson et al., 2016;
Frigola et al., 2018).

4.5 Glaciers and ice caps

265 Glaciers and ice caps have a decadal to century timescale response and are vulnerable to small perturbations in the climate
forcing. For the highest forcing scenarios MMCP-break, MMCP8.5 and MMCP-feedback, the glaciers and ice caps melt away
entirely in the coming 1000 to 2000 years. Under scenario MMCP2.6 it takes up to 3000 years before the glaciers and ice caps
lose most of their ice volume. On the multi-millennial timescale, the differences in the glaciers and ice caps contribution to
sea-level change are very small compared to the other components with total contribution between 0.23 and 0.24 m for any of
the forcing scenarios.



270 5. Global mean sea-level change

Total GMSL changes in our experiments range between 9.2 m and 37.4 m at the end of the 10,000 year experiments (Figure 5a). Moreover, the rates of GMSL rise vary substantially between the different scenarios and over time. We investigate the relation between cumulative CO₂ emissions and GMSL change, somewhat similar to the notion of a relationship between global warming and cumulative CO₂ emissions by a certain time, expressed as the Transient Climate Response to cumulative carbon Emissions (TCRE: Matthews et al., 2018) or the Multi-millennial Climate Response to cumulative carbon Emissions (MCRE: Frölicher and Paynter, 2015). In Fig. 5b, the realised GMSL rise after each 1000 years is shown as a function of the total cumulative CO₂ emission after 2000 AD for each experiment.

In case total cumulative CO₂ emission exceed 2000 GtC, GMSL change rates are highest during the first 2 millennia. However, when cumulative CO₂ emissions stay below 200 GtC (MMCP2.6), the peak rates in GMSL change occur only 4000 to 8000 years from now due to slow melting of the GrIS and ensuing feedbacks. A total sea level rise of 8.8 m is achieved after 10,000 years, even though CO₂ emissions already ceased before the mid 21st century. For the other experiments, the rate of sea-level change decreases with time. All experiments approach a semi equilibrium after 10,000 years (Figure 5a). The rate of global sea-level change is then still positive for all simulations, albeit reduced to about 0.05 m per century for the experiment with the largest cumulative CO₂ emission (MMCP-feedback). This reflects the long equilibration time for the ice sheets and the ocean within the coupled climate system to adapt to temperature changes.

In our simulations, Greenland is the largest contributor to GMSL rise up to a cumulative CO₂ emission of 2000 GtC. The grounding line of the West Antarctic ice sheet (WAIS) retreats several 100 km inland using scenario MMCP2.6 and MMCP4.5. The WAIS disintegrates completely for cumulative CO₂ emissions around 2000 GtC, but East Antarctica still remains mostly unaffected. For higher cumulative emissions, marine-based parts of East Antarctica start to disintegrate and Antarctica becomes the largest source to GMSL rise.

The total sea-level rise after 10,000 years includes the (nearly) entire melt of the Greenland ice sheet as well as glaciers and ice caps. The spread is largest for the Antarctic contribution taken over all scenarios, ranging from 1.6 to 27 m (corresponding to ~200 to ~5000 GtC cumulative CO₂ emissions after 2000 AD). The contribution from thermal expansion and haline contraction ranges between 0.4 and 3 m. Table 1 gives an overview of the sea-level contribution and the relative share to GMSL of each component for all forcing scenarios.

6. Long-term sea level rise in the light of the geological record

An interesting test for our sea-level change projections can be provided by the geological record of sea-level high stands as a function of the inferred atmospheric carbon dioxide concentration. Estimates of paleo sea level variations range from a lowstand of -120 m for CO₂ concentrations around 180 ppmv to a highstand of +65 m for CO₂ concentrations up to 1200 ppmv



300 (Alley et al., 2005, Foster and Rohling, 2013). Such data suggest a linear sigmoidal behaviour for (semi)-equilibrated periods
in the past, where sea-level high stands changes abruptly for deviations of the greenhouse gas forcing from the pre-industrial
due to the build-up of the large northern hemisphere ice sheets during glacial periods and the total melting of the Greenland
and Antarctic ice sheet for a high CO₂ greenhouse world during the Eocene. Assuming that our climate (and sea-level change)
components are nearly equilibrated after 10,000 years, we compare our GMSL changes with the geological archive (Foster and
305 and Rohling, 2013). For this comparison, it is important to realise that the time scale of carbon input in the atmosphere may
be a critical parameter as the peak atmospheric CO₂ concentration shows a strong dependence on the emission pathway.
However, simulations with biogeochemical models show that the mean atmospheric CO₂ concentration over multiple kyr is
mostly independent from the duration of carbon release (Zeebe and Zachos, 2013). Moreover, on a multi-centennial timescale,
global mean temperature perturbations converge to a single value, suggesting a pathway independence of cumulative emissions
310 (Zickfeld et al., 2012, Rogelj et al., 2016). We therefore opt to average the CO₂ concentration over the next 10,000 years,
suggesting that the mean concentration represents the multi-millennial temperature change at best.

Figure 6 shows the GMSL change after 10,000 years as a function of the mean atmospheric CO₂ compared with the geological
archive. We compared a piecewise linear fit of the data obtained in this paper (red line) with the best fit of the geological data
(blue line, polynomial with exponent 2; data from Foster and Rohling, 2013). Both of the fitted lines compare quite well. There
315 is a somewhat larger discrepancy for the highest CO₂ concentration, but the (near) total melting of all ice on Earth for a mean
CO₂ concentration of 1200 ppmv is based on only a few geological data points. Moreover, a further upward GMSL evolution
after 10,000 years cannot be excluded in our experiments due to a further adjustment of the AIS and a continued response of
the deep ocean to the surface warming and resulting thermal expansion.

7. Discussion

320 Glaciers and ice caps are the second largest contributor to present-day GMSL rise (after the thermosteric component) and will
continue to be a major source of sea-level rise during the next century (WCRP Global Sea Level Budget Group, 2018). At the
end of the 21st century, the global glacier volume is projected to decrease between 21 % (MMCP2.6) and 24 % (MMCP8.5).
The contribution to GMSL from glaciers and ice caps melting generally corroborate the findings by Hock et al. (2019), who
found that by the end of the 21st century mountain glaciers and ice caps lose between 11-25 % (RCP2.6) and 25-47 % (RCP8.5)
325 of their volume. For scenario MMCP8.5, our results are below the average estimates at the end of the 21st century because of
the rather low climate sensitivity in LOVECLIM. At the end of the simulations, the lower sensitivity of our glacier model to
the high forcing scenarios is irrelevant and glaciers and ice caps will lose 96 - 100 % of their volume for any of the forcing
scenarios. Raper and Braithwaite (2006) and Goelzer et al. (2012) found that glaciers and ice caps disappear completely for a
global warming of around 4°C by the end of the third millennium.



330 GMSL rise due to thermal expansion and haline contraction has a sensitivity of 0.27 to 0.68 m per °C, where the stronger
forcing scenarios have the higher contribution due to the additional effect of haline contraction. Levermann et al. (2013)
identified a similar linear relation between thermal expansion and global mean temperatures of 0.2 to 0.63 m per °C.
Hieronymus (2019) assessed several coupled climate models and found an updated sensitivity of 0.51 to 0.83 m per °C of
surface warming. The higher sensitivity is present in climate models that show an increase in AMOC strength. However, the
335 AMOC strength is (temporarily) decreasing in our experiments, especially in the simulations where the GrIS is melting fast.
Therefore, the higher sensitivity reported by Hieronymus (2019) might be an overestimation in future scenarios where the ice
sheets will melt strongly, due to the neglect of ice sheet-ocean interactions.

The largest (scenario-based) uncertainty in future multi-millennial sea level rise comes from the polar ice sheets. In our
simulations, melting of the entire GrIS takes about 10,000 years for a local annual mean temperature anomaly of 2°C with
340 respect to 1970-2000 AD. In higher scenarios, the GrIS needs between 8000 years for MMCP4.5 with a mean SAT anomaly
of 5.1°C and 2000 years for MMCP-feedback with a mean SAT anomaly of 9.8 °C, to disintegrate entirely. Robinson et al.
(2012) found the temperature threshold for melting the entire Greenland ice sheet to lie between 0.8 and 3.2°C, with a long
decay time for temperatures close to this threshold. Since the temperature anomaly in scenario MMCP2.6 is close to this
threshold, it takes about 10,000 years in our simulations to melt the entire GrIS. According to Aschwanden et al. (2019), the
345 GrIS will lose between 72 % and 100 % of its volume by the end of the next millenium, using an extreme melt forcing and
neglecting the temporarily cooling effect of a reduced AMOC. Other studies found that the GrIS could disappear in less than
3000 years for a constant CO₂ forcing exceeding 1100 ppmv (Alley et al., 2005, Driesschaert et al., 2007, Huybrechts et al.,
2011), in the same range as our simulations even though the results are not entirely comparable owing to a different time
evolution of the CO₂ and temperature forcing.

350 The marine-based WAIS is considered the most vulnerable part of the AIS and collapses for cumulative CO₂ emission
exceeding ~1100 GtC. The Wilkes subglacial basin in East Antarctica becomes ice-free in scenarios MMCP-break, MMCP8.5
and MMCP-feedback. The Aurora Basin also loses its ice cover for scenario MMCP-feedback. The ice sheet respectively
contributes 12 m, 19.6 m and 27 m to sea level following scenarios MMCP-break, MMCP8.5 and MMCP-feedback (Figure
4). Our numbers for MMCP8.5 are comparable to the study by Golledge et al. (2015), equally based on an extension of the
355 ECP8.5 scenario with constant forcing after 2300 AD. They found that AIS retreat over the Wilkes and Aurora basins would
contribute up to 11.4 m to GMSL after 5000 years and 15.7 m after 50,000 years. In the simulations of Winkelmann et al.
(2015), the grounding line retreats significantly along the WAIS for a cumulative emission of 1000 GtC, while in East
Antarctica the retreat is most rapid for the Wilkes and Aurora subglacial basins and initiates for a cumulative CO₂ emission of
2500 GtC. Considering a cumulative CO₂ emission of 10,000 GtC, Winkelmann et al. (2015) even found that the Antarctic ice
360 sheet could nearly disappear entirely. However, that is an extreme scenario at the upper end of potential carbon reserves and
resources available for combustion, which we did not consider in the present paper.



365 Even though the resolution of the ice sheet models and the climate model is relatively coarse, especially to simulate the retreat
along the outlet glaciers in Greenland and the grounding line retreat in the most sensitive Antarctic regions such as Thwaites
or Pine Island glaciers in West Antarctica, the model is performing quite well to simulate the ice sheet response on the millennial
timescale. Marine terminating glaciers along the Greenland ice sheet will retreat in the coming decades and the SMB will
dominate the Greenland mass loss. The Antarctic ice sheet model run at 20 km resolution is too coarse to simulate fast flowing
glaciers in great detail and the omission of sub-grid scale mechanisms makes the model less sensitive on the short-term to
basal melting (Levermann et al., 2020, Seroussi et al., 2020). However, the grounding line retreats on land in Antarctica for
most scenarios and also here, the influence of SMB processes becomes more important. Because of the rather low contribution
370 of the AIS to sea-level by 2300 AD for scenario MMCP2.6 and the lower sensitivity to grounding line retreat compared to
other ice sheet models (Levermann et al., 2020), we assume that our lowest sea-level change value is a conservative estimate.

It should be noted that our ice sheet models do not include hydrofracturing. Hydrofracturing may significantly speed up
Antarctic ice sheet decay as achieved by the Marine Ice Cliff Instability (MICI) mechanism (Pollard et al., 2015). DeConto
and Pollard (2016) find Antarctic ice sheet volume losses equivalent to a freshwater input into the surrounding ocean in excess
375 of 1 Sv, much larger than the peak freshwater input in our simulations of 0.15 Sv. However, the MICI is controversial for its
large contribution to sea level already at the end of the 21st century (e.g. Edwards et al., 2019).

Clark et al. (2016) found the AIS to be the largest contributor to sea level rise after 10,000 years for all of the scenarios they
considered. Moreover, it is suggested that the sensitivity of GMSL change to atmospheric CO₂ lowers for higher cumulative
CO₂ emissions with a logarithmic relation between both. For the first 2 millennia, our results show a similar behaviour, but at
380 the end of the 10,000 years simulations, GMSL increased more for the higher emission scenarios and a stronger non-linear
relationship between GMSL and cumulative CO₂ emissions was established. Part of the discrepancy can be explained by the
difference between scenario MMCP8.5 and MMCP-feedback. Both scenarios assume the same peak CO₂ values, but the latter
adds more carbon to the atmosphere after 10,000 years due to the methane emission feedback. Another difference with our
experiments is that we include the albedo-temperature feedback, which gains importance once the Antarctic ice sheet retreats
385 inland.

Oppositely to previous modelling studies investigating the Antarctic ice sheet evolution on a multi-millennial timescale
(Winkelmann et al., 2015, DeConto and Pollard, 2016, Clark et al., 2016), we include the two-way feedbacks between the ice
sheets, the atmosphere and the ocean. Large amounts of freshwater – due to melting of the ice shelves and grounded ice from
Antarctica – enter the Southern Ocean and impact on Antarctic Bottom Water (AABW) and sea ice formation (Swingedouw
390 et al., 2008, Goelzer et al., 2016a, Goelzer et al., 2016b). On the other hand, freshwater fluxes from melting the GrIS reduce
strongly the NADW formation and weaken the AMOC. The interhemispheric see-saw effect is understood as weakening
NADW formation leading to a reduced transport of cold water to the Antarctic leading to a warming of the Antarctic continent
(Stocker, 1998). However, in our future warming simulations, the AIS is also melting and freshwater fluxes act as a negative



395 feedback by limiting the ocean temperature increase locally (Figure 11). The observed limited warming in our simulations is
supported by a study from Swingedouw et al. (2009) who found regional cooling of up to 10 °C following a freshwater release
of 1 Sv in the Southern ocean. In contrast to other studies that suggest an increase in sea-ice area due to large freshwater pulses
(Swingedouw et al., 2008; Goelzer et al., 2016b) where the ocean stratification increases beneath the ocean surface leading
ultimately to ice shelf melting at depth (Golledge et al., 2014). This positive feedback is not observed in our simulations, where
the sea-ice area (and volume) declines strongly in all our experiments and almost all sea-ice disappears for the three highest
400 forcing scenarios at the end of the first millennium (Figure 9).

8. Conclusions

In this paper we have assessed multi-millennial sea-level change projections having fully interactive ice sheet components as
obtained within the Earth System Model of Intermediate Complexity LOVECLIM. Global mean sea level is shown to
continuously rise during the next 10,000 years for all scenarios considered. These build further on IPCC RCP/ECP scenarios
405 with emission pathways ranging from temporarily negative emissions to burning ~5000 GtC with the addition of a methane
emission feedback. The sea-level rise is thus found to be irreversible on a 10,000 year time scale, even for the lowest forcing
scenario based on extending scenario RCP2.6 with zero emissions.

The interactive nature of our model study on the multi-millennial timescale is important to simulate most climatic feedbacks
in the real world in an accurate way. Ice sheet-ocean interactions results in temporarily large perturbations in the ocean
circulation with freshwater fluxes from the GrIS leading to a strongly reduced AMOC strength and local cooling. Apart from
410 the local cooling effect and its influence on atmospheric temperatures in the vicinity of the Greenland ice sheet, our findings
suggest that the reduced AMOC also lowers the contribution from the steric component to GMSL. Freshwater fluxes from the
AIS lead to reduced oceanic warming in the vicinity of Antarctica and relatively low basal melt rates. Ice sheet - atmosphere
interactions on a multi-millennial timescale are important to take into account because of the SMB-elevation feedback that
415 sets-in when the ice sheet starts to melt and the surface elevation decreases. The strong albedo-temperature feedback initiates
when the ice sheets retreat on land, where temperatures increase due to an increase in the tundra-like surface type (in addition
to the effect of a reduced sea-ice area). As a consequence, surface melting accelerates once a critical area of land becomes
ice-free.

It is found that the Greenland ice sheet will melt entirely over the next 10,000 years, but the rate of sea-level rise is determined
420 by the forcing scenario. Oppositely, the fate of the Antarctic ice sheet is largely dependent on the future greenhouse gas forcing
scenario considered. For the lowest forcing scenario, there is only a limited retreat of the grounding line in West Antarctica
and the East Antarctic ice sheet remains mostly unaffected, resulting in a limited sea-level contribution of 1.6 m. For the
highest forcing scenarios, the West Antarctic ice sheet will collapse entirely and there is significant marginal ice sheet retreat
along the East Antarctic ice sheet with a total volume loss of around 27 m SLE. The combined contribution of thermal



425 expansion and haline contraction continues to contribute to sea level rise as long as there is a freshwater influx, even though
 the bulk of the oceanic heat increase takes place in the first centuries after the steep rise in temperatures. It is the only
 component contributing to sea level that reached a peak during the coming millennia and decreases slowly towards the end of
 the simulations (only for the two lowest scenarios) following a slight global cooling trend after a few thousand years. Glaciers
 and ice caps are the smallest component in the sea level budget and disappear relatively fast during the coming centuries.

430 We have identified the existence of a threshold in total cumulative CO₂ emissions for which GMSL is dominated by melting
 of the Greenland ice sheet or by GMSL contributions from the Antarctic ice sheet. In our simulations, GMSL rise is dominated
 by melting of the Greenland ice sheet for a total cumulative CO₂ emission of up to 1100 GtC (after 2000 AD). Under these
 scenarios, GMSL is found to quasi stabilize between 8.8 and 15 m above current levels. For the higher emission scenarios, the
 AIS contribution exceeds the GrIS contribution after 1000 years due to grounding line retreat and surface melting in East
 435 Antarctica and total GMSL rise after 10,000 years ranges between 22 and 38 m. Near the end of the simulations, the rate of
 sea-level change decreases to values below 0.05 m per century for all forcing scenarios and sea-level approaches a semi-
 equilibrated state.

Appendix A: Construction of the carbon dioxide concentration scenarios

We assume that an impulse response function (IRF) represents the time-dependent abundance of a gas after an additional
 440 emission pulse (Joos et al., 2013; Maier-Reimer and Hasselmann, 1987). After the peak concentration, the CO₂ concentration
 decreases exponentially reaching a short-term equilibrium CO₂^{equi_s} (after 1000 years) and a long-term equilibrium CO₂^{equi_l}
 (after 10,000 years) based on Eq. (1) and Eq. (2) (Solomon et al., 2009). The time constants used for the two exponentials do
 not have a process based meaning, but are fitting parameters to best represent the wide range of IRFs present in the literature.
 The peak airborne fraction (AF^{peak}), the short-term stabilization level CO₂^{equi_s} and the long-term stabilisation level CO₂^{equi_l} (*
 445 can be replaced by l and s in Eq. (2)) represent the different theoretical neutralization processes.

$$CO_2(t) = CO_2^{equi_l} + \left[(CO_2^{peak} - CO_2^{equi_s})e^{-\lambda_s t} + (CO_2^{equi_l} - CO_2^{equi_s})e^{-\lambda_l t} \right] \quad (1)$$

Where: CO₂^{equi_s} = equilibrium CO₂ concentration after 1000 years

CO₂^{equi_l} = equilibrium CO₂ concentration after 10,000 years

CO₂^{peak} = peak CO₂ concentration

λ_s = short term decay rate

λ_l = long term decay rate

t = time (between peak concentration and 12,000 AD)

$$450 \quad CO_2^{equi_s} = \frac{AF^{equi_s}}{AF^{peak}} (CO_2^{peak} - CO_2^0) + CO_2^0 \quad (2)$$

455 Where: CO₂⁰ = 280 ppmv



$AF^{\text{equi}*}$ = equilibrium airborne fraction

AF^{peak} = peak airborne fraction

460 The instantaneous or peak airborne fraction (AF^{peak}) is the atmospheric CO₂ peak concentration as a percentage of the total
released CO₂ (Archer and Brovkin, 2008). AF^{equi} measures the fraction of emitted CO₂ that remains in the atmosphere after
1000 years (AF^{equi_s}) and 10,000 years (AF^{equi_l}), respectively. The main principle is that the more CO₂ is emitted in the
atmosphere, the lower the capacity of the ocean to buffer the excess of carbon due to the limited size of the ocean (Archer et
al., 2009a). Dissolved carbon in the ocean consists of bicarbonate (HCO₃⁻) and carbonate ions (CO₃²⁻). The latter buffers the
ocean against CO₂ invasion, but is less abundant than bicarbonate. Depletion of the bicarbonate ions starts with increasing
465 atmospheric CO₂ concentrations. As a consequence, the buffering capacity of the ocean decreases with higher CO₂ atmospheric
injections (Archer and Brovkin, 2008).

The airborne fractions are chosen in accordance with the values present in the literature (Table A1) and extrapolated for the
scenarios that do not correspond to the CO₂ emission pulses (Table A2). The peak airborne fraction after a pulse injection of
470 CO₂ is 100 % and therefore not completely comparable with the more gradual injections as assumed by the MMCP scenarios.
Therefore, these peak airborne fractions are scaled to the peak airborne fractions for a slower injection of CO₂ where the peak
atmospheric CO₂ value is between 50 and 70 % of the real atmospheric CO₂ emissions (Archer and Brovkin, 2008).

Author contribution

475 PH and HG designed the experiments and JVB carried them out. HG and PH developed the model code. JVB prepared the
manuscript with contributions from all co-authors.

Acknowledgements

We acknowledge support through the Belgian Federal Science Policy Office within its Research Programme on Science for a
Sustainable Development under contract SD/CS/06A (iCLIPS) and the Belgian National Agency for Radioactive Waste and
enriched Fissile Material (ONDRAF/ NIRAS). Heiko Goelzer has received funding from the programme of the Netherlands
480 Earth System Science Centre (NESSC), financially supported by the Dutch Ministry of Education, Culture and Science (OCW)
under grant no. 024.002.001.



485 References

- Alley, R. B. and Whillans, I. M.: Response of the East Antarctica ice sheet to sea-level rise, *J. Geophys. Res.*, 89, 6487–6493, <https://doi.org/10.1029/JC089iC04p06487>, 1984.
- Alley, R. B., Clark, P. U., Huybrechts, P. and Joughin, I.: Ice-Sheet and Sea-Level Changes, *Science*, 310, 456–460, <https://doi.org/10.1126/science.1114613>. 2005.
- 490 Applegate, P. J., Parizek, B. R., Nicholas, R. E., Alley, R. B. and Keller, K.: Increasing temperature forcing reduces the Greenland Ice Sheet’s response time scale, *Clim. Dyn.*, 45, 2001–2011, <https://doi.org/10.1007/s00382-014-2451-7>, 2015.
- Archer, D. and Brovkin, V.: The millennial atmospheric lifetime of anthropogenic CO₂, *Clim. Change*, 90, 283–297, <https://doi.org/10.1007/s10584-008-9413-1>, 2008.
- Archer, D., Eby, M., Brovkin, V., Ridgwell, A., Cao, L., Mikolajewicz, U., Caldeira, K., Matsumoto, K., Munhoven, G.,
495 Montenegro, A. and Tokos, K.: Atmospheric Lifetime of Fossil Fuel Carbon Dioxide, *Annu. Rev. Earth Planet. Sci.*, 37, 117–134, <https://doi.org/10.1146/annurev.earth.031208.100206>, 2009a.
- Archer, D., Buffett, B. and Brovkin, V.: Ocean methane hydrates as a slow tipping point in the global carbon cycle, *Proc. Natl. Acad. Sci. USA.*, 106, 20596–20601, <https://doi.org/10.1073/pnas.0800885105>, 2009b.
- Aschwanden, A., Fahnstock, M.A., Truffer, M., Brinkerhoff, D.J., Hock, R., Khroulev, C., Mottram R. and Khan, S.A.:
500 Contribution of the Greenland Ice sheet to sea level over the next millennium, *Sci. Adv.*, 5, <https://doi.org/10.1126/sciadv.aav9396>, 2019.
- Barthel, A., Agosta, C., Little, C. M., Hattermann, T., Jourdain, N. C., Goelzer, H., Nowicki, S., Seroussi, H., Straneo, F., and Bracegirdle, T. J.: CMIP5 model selection for ISMIP6 ice sheet model forcing: Greenland and Antarctica, *The Cryosphere*, 14, 855–879, <https://doi.org/10.5194/tc-14-855-2020>, 2020.
- 505 Bulthuis, K., Arnst, M., Sun, S. and Pattyn, F.: Uncertainty quantification of the multi-centennial response of the Antarctic ice sheet to climate change, *Cryosph.*, 13, 1349–1380, doi.org/10.5194/tc-13-1349-2019, 2019.
- Calov, R., Beyer, S., Greve, R., Beckmann, J., Willeit, M., Kleiner, T., Rückamp, M., Humbert, A. and Ganopolski, A.: Simulation of the future sea level contribution of Greenland with a new glacial system model, *The Cryosphere*, 12, 3097–3121, <https://doi.org/10.5194/tc-12-3097-2018>, 2018.
- 510 Charbit, S., Paillard, D. and Ramstein, G.: Amount of CO₂ emissions irreversibly leading to the total melting of Greenland, *Geophys. Res. Lett.*, 35, 1–5, <https://doi.org/10.1029/2008GL033472>, 2008.
- Church, J. A. and White, N. J.: Sea-Level Rise from the Late 19th to the Early 21st Century, *Surv. Geophys.*, 32, 585–602, <https://doi.org/10.1007/s10712-011-9119-1>, 2011.
- Ciais, P., Sabine, C., Bala, G., Bopp, L., Brovkin, V., Canadell, J., Chhabra, A., DeFries, R., Galloway, J., Heimann, M., Jones,
515 C., Quéré, C. Le, Myneni, R. B., Piao, S. and Thornton, P.: Carbon and Other Biogeochemical Cycles. In: *Climate Change 2013: The Physical Science Basis. Contribution of working group I to the Fifth Assessment Report of the Intergovernmental*



- Panel on Climate Change [Stocker, T.F., D. Qin, G.-K. Plattner, M. Tignor, S.K. Allen, J. Boschung, A. Nauels, Y. Xia, V. Bex and P.M. Midgley (eds.)], Cambridge University Press, Cambridge, United Kingdom and New York, NY, USA, 2013
- 520 Clark, P. U., Shakun, J. D., Marcott, S. A., Mix, A. C., Eby, M., Kulp, S., Levermann, A., Milne, G. A., Pfister, P. L., Santer, B. D., Schrag, D. P., Solomon, S., Stocker, T. F., Strauss, B. H., Weaver, A. J., Winkelmann, R., Archer, D., Bard, E., Goldner, A., Lambeck, K., Pierrehumbert, R. T. and Plattner, G. K.: Consequences of twenty-first-century policy for multi-millennial climate and sea-level change, *Nat. Clim. Chang.*, 6, 360–369, <https://doi.org/10.1038/nclimate2923>, 2016.
- DeConto, R. M. and Pollard, D.: Contribution of Antarctica to past and future sea-level rise, *Nature*, 531, 591–597, <https://doi.org/10.1038/nature17145>, 2016.
- 525 Dickens, G. R.: Down the Rabbit Hole: toward appropriate discussion of methane release from gas hydrate systems during the Paleocene-Eocene thermal maximum and other past hyperthermal events, *Clim. Past*, 7, 831–846, <https://doi.org/10.5194/cp-7-831-2011>, 2011.
- Driesschaert, E., Fichefet, T., Goosse, H., Huybrechts, P., Janssens, I., Mouchet, A., Munhoven, G., Brovkin, V. and Weber, S. L.: Modeling the influence of Greenland ice sheet melting on the Atlantic meridional overturning circulation during the next
530 millennia, *Geophys. Res. Lett.*, 34, 1–5, <https://doi.org/10.1029/2007GL029516>, 2007.
- Eby, M., Zickfeld, K., Montenegro, A., Archer, D., Meissner, K. J. and Weaver, A. J.: Lifetime of Anthropogenic Climate Change: Millennial Time Scales of Potential CO₂ and Surface Temperature Perturbations, *J. Clim.*, 22, 2501–2511, <https://doi.org/10.1175/2008JCLI2554.1>, 2009.
- Edwards, T. L., Brandon, M. A., Durand, G., Edwards, N. R., Golledge, N. R., Holden, P. B., Nias, I. J., Payne, A. J., Ritz, C.
535 and Wernecke, A.: Revisiting Antarctic ice loss due to marine ice-cliff instability, *Nature*, 566, 58–64, <https://doi.org/10.1038/s41586-019-0901-4>, 2019.
- Farinotti, D., Huss, M., Fürst, J. J., Landmann, J., Machguth, H., Maussion, F. and Pandit, A.: A consensus estimate for the ice thickness distribution of all glaciers on Earth, *Nat. Geosci.*, 12, 168–173, <https://doi.org/10.1038/s41561-019-0300-3>, 2019.
- Feistel, R.: Extended equation of state for seawater at elevated temperature and salinity, *Desalination*, 250, 14–18,
540 <https://doi.org/10.1016/j.desal.2009.03.020>, 2010.
- Fettweis, X., Franco, B., Tedesco, M., van Angelen, J. H., Lenaerts, J. T. M., van den Broeke, M. R., and Gallée, H.: Estimating the Greenland ice sheet surface mass balance contribution to future sea level rise using the regional atmospheric climate model MAR, *The Cryosphere*, 7, 469–489, <https://doi.org/10.5194/tc-7-469-2013>, 2013.
- Foster, G. L. and Rohling, E. J.: Relationship between sea level and climate forcing by CO₂ on geological timescales, *Proc. Natl. Acad. Sci. USA*, 110, 1209–1214, <https://doi.org/10.1073/pnas.1216073110>, 2013.
- 545 Frigola, A., Prange, M., and Schulz, M.: Boundary conditions for the Middle Miocene Climate Transition (MMCT v1.0), *Geosci. Model Dev.*, 11, 1607–1626, <https://doi.org/10.5194/gmd-11-1607-2018>, 2018.
- Frölicher, T.L. and Paynter, D. J.: Extending the relationship between global warming and cumulative carbon emissions to multi-millennial timescales, *Environ. Res. Lett.*, 10, 075002, <https://doi.org/10.1088/1748-9326/10/7/075002>, 2015.
- 550 Gasson, E., DeConto, R. M., Pollard, D. and Levy, R. H.: Dynamic Antarctic ice sheet during the early to mid-Miocene, *Proc.*



- Natl. Acad. Sci. USA, 113, 3459–3464, <https://doi.org/10.1073/pnas.1516130113>, 2016.
- Gillett, N. P., Arora, V. K., Zickfeld, K., Marshall, S. J. and Merryfield, W. J.: Ongoing climate change following a complete cessation of carbon dioxide emissions, *Nat. Geosci.*, 4, 83–87, <https://doi.org/10.1038/ngeo1047>, 2011.
- 555 Goelzer, H., Huybrechts, P., Raper, S. C. B., Loutre, M. F., Goosse, H. and Fichefet, T.: Millennial total sea-level commitments projected with the Earth system model of intermediate complexity LOVECLIM, *Environ. Res. Lett.*, 7, 045401, <https://doi.org/10.1088/1748-9326/7/4/045401>, 2012.
- Goelzer, H., Huybrechts, P., Loutre, M.-F., and Fichefet, T.: Impact of ice sheet meltwater fluxes on the climate evolution at the onset of the Last Interglacial, *Clim. Past*, 12, 1721–1737, <https://doi.org/10.5194/cp-12-1721-2016>, 2016a.
- 560 Goelzer, H., Huybrechts, P., Loutre, M.-F., and Fichefet, T.: Last Interglacial climate and sea-level evolution from a coupled ice sheet–climate model, *Clim. Past*, 12, 2195–2213, <https://doi.org/10.5194/cp-12-2195-2016>, 2016b.
- Goelzer, H., Coulon, V., Pattyn, F., de Boer, B., and van de Wal, R.: Brief communication: On calculating the sea-level contribution in marine ice-sheet models, *The Cryosphere*, 14, 833–840, <https://doi.org/10.5194/tc-14-833-2020>, 2020a.
- 565 Goelzer, H., Nowicki, S., Payne, A., Larour, E., Seroussi, H., Lipscomb, W. H., Gregory, J., Abe-Ouchi, A., Shepherd, A., Simon, E., Agosta, C., Alexander, P., Aschwanden, A., Barthel, A., Calov, R., Chambers, C., Choi, Y., Cuzzone, J., Dumas, C., Edwards, T., Felikson, D., Fettweis, X., Golledge, N. R., Greve, R., Humbert, A., Huybrechts, P., Le clec'h, S., Lee, V., Leguy, G., Little, C., Lowry, D. P., Morlighem, M., Nias, I., Quiquet, A., Rückamp, M., Schlegel, N.-J., Slater, D., Smith, R., Straneo, F., Tarasov, L., van de Wal, R., and van den Broeke, M.: The future sea-level contribution of the Greenland ice sheet: a multi-model ensemble study of ISMIP6, *The Cryosphere Discuss.*, <https://doi.org/10.5194/tc-2019-319>, in review, 2020b.
- 570 Golledge, N. R., Menviel, L., Carter, L., Fogwill, C. J., England, M. H., Cortese, G. and Levy, R.H.: Antarctic contribution to meltwater pulse 1A from reduced Southern Ocean overturning, *Nature Commun.*, 5, 5107, <https://doi.org/10.1038/ncomms6107>, 2014.
- Golledge, N. R., Kowalewski, D. E., Naish, T. R., Levy, R. H., Fogwill, C. J. and Gasson, E. G. W.: The multi-millennial Antarctic commitment to future sea-level rise, *Nature*, 526, 421–425, <https://doi.org/10.1038/nature15706>, 2015.
- 575 Golledge, N. R.: Long-term projections of sea-level rise from ice sheets, *Wiley Interdiscip Rev Clim Change*, 11, e634, <https://doi.org/10.1002/wcc.634>, 2020.
- Goosse, H. and Fichefet, T.: Importance of ice-ocean interactions for the global ocean circulation: A model study, *J. Geophys. Res. Ocean.*, 104, 23337–23355, <https://doi.org/10.1029/1999jc900215>, 1999.
- 580 Goosse, H., Brovkin, V., Fichefet, T., Haarsma, R., Huybrechts, P., Jongma, J., Mouchet, A., Selten, F., Barriat, P.-Y., Campin, J.-M., Deleersnijder, E., Driesschaert, E., Goelzer, H., Janssens, I., Loutre, M.-F., Morales Maqueda, M. A., Opsteegh, T., Mathieu, P.-P., Munhoven, G., Pettersson, E. J., Renssen, H., Roche, D. M., Schaeffer, M., Tartinville, B., Timmermann, A., and Weber, S. L.: Description of the Earth system model of intermediate complexity LOVECLIM version 1.2, *Geosci. Model Dev.*, 3, 603–633, <https://doi.org/10.5194/gmd-3-603-2010>, 2010.
- Griffis, T. J., Chen, Z., Baker, J. M., Wood, J. D., Millet, D. B., Lee, X., Venterea, R. T. and Turner, P. A.: Nitrous oxide emissions are enhanced in a warmer and wetter world, *Proc. Natl. Acad. Sci. USA*, 114, 12081–12085,



- 585 <https://doi.org/10.1073/pnas.1704552114>, 2017.
- Hasselmann, K., Latif, M., Hooss, G., Azar, C., Edenhofer, O., Jaeger, C. C., Johannessen, O. M., Kemfert, C., Welp, M. and Wokaun, A.: The Challenge of Long-Term Climate Change, *Science*, 302, 1923–1925, <https://doi.org/10.1126/science.1090858>, 2003.
- Hay, C. C., Morrow, E., Kopp, R. E. and Mitrovica, J. X.: Probabilistic reanalysis of twentieth-century sea-level rise, *Nature*, 590 517, 481–484, <https://doi.org/10.1038/nature14093>, 2015.
- Hieronymus, M.: An update on the thermosteric sea level rise commitment to global warming, *Environ. Res. Lett.*, 14, 054018, <https://doi.org/10.1088/1748-9326/ab1c31>, 2019.
- Hock, R., Bliss, A., Marzeion, B., Giesen, R. H., Hirabayashi, Y., Huss, M., Radic, V. and Slangen, A. B. A.: GlacierMIP - A model intercomparison of global-scale glacier mass balance models and projections, *J. Glaciol.*, 65, 453–467, 595 <https://doi.org/10.1017/jog.2019.22>, 2019.
- Huybrechts, P.: Glaciological Modelling of the Late Cenozoic East Antarctic Ice Sheet: Stability or Dynamism?, *Geogr. Ann. Ser. A, Phys. Geogr.*, 75, 221–238, <https://doi.org/10.1080/04353676.1993.11880395>, 1993.
- Huybrechts, P. and De Wolde, J.: The Dynamic Response of the Greenland and Antarctic Ice Sheets to Multiple-Century Climatic Warming, *J. Clim.*, 12, 2169–2188, [https://doi.org/10.1175/1520-0442\(1999\)012<2169:tdrotg>2.0.co;2](https://doi.org/10.1175/1520-0442(1999)012<2169:tdrotg>2.0.co;2), 1999.
- 600 Huybrechts, P., Goelzer, H., Janssens, I., Driesschaert, E., Fichet, T., Goosse, H. and Loutre, M. F.: Response of the Greenland and Antarctic Ice Sheets to Multi-Millennial Greenhouse Warming in the Earth System Model of Intermediate Complexity LOVECLIM, *Surv. Geophys.*, 32, 397–416, <https://doi.org/10.1007/s10712-011-9131-5>, 2011.
- Huss, M. and Hock, R.: A new model for global glacier change and sea-level rise, *Front. Earth Sci*, 3, <https://doi.org/10.3389/feart.2015.00054>, 2015.
- 605 Jackson, L. P. and Jevrejeva, S.: A probabilistic approach to 21st century regional sea-level projections using RCP and High-end scenarios, *Glob. Planet. Change*, 146, 179–189, <https://doi.org/10.1016/j.gloplacha.2016.10.006>, 2016.
- Joos, F., Roth, R., Fuglestedt, J. S., Peters, G. P., Enting, I. G., von Bloh, W., Brovkin, V., Burke, E. J., Eby, M., Edwards, N. R., Friedrich, T., Frölicher, T. L., Halloran, P. R., Holden, P. B., Jones, C., Kleinen, T., Mackenzie, F. T., Matsumoto, K., Meinshausen, M., Plattner, G.-K., Reisinger, A., Segschneider, J., Shaffer, G., Steinacher, M., Strassmann, K., Tanaka, K., 610 Timmermann, A., and Weaver, A. J.: Carbon dioxide and climate impulse response functions for the computation of greenhouse gas metrics: a multi-model analysis, *Atmos. Chem. Phys.*, 13, 2793–2825, <https://doi.org/10.5194/acp-13-2793-2013>, 2013.
- Kirschke, S., Bousquet, P., Ciais, P., Saunoy, M., Canadell, J. G., Dlugokencky, E. J., Bergamaschi, P., Bergmann, D., Blake, D. R., Bruhwiler, L., Cameron-Smith, P., Castaldi, S., Chevallier, F., Feng, L., Fraser, A., Heimann, M., Hodson, E. L., 615 Houweling, S., Josse, B., Fraser, P. J., Krummel, P. B., Lamarque, J. F., Langenfelds, R. L., Le Quéré, C., Naik, V., O’doherly, S., Palmer, P. I., Pison, I., Plummer, D., Poulter, B., Prinn, R. G., Rigby, M., Ringeval, B., Santini, M., Schmidt, M., Shindell, D. T., Simpson, I. J., Spahni, R., Steele, L. P., Strode, S. A., Sudo, K., Szopa, S., Van Der Werf, G. R., Voulgarakis, A., Van Weele, M., Weiss, R. F., Williams, J. E. and Zeng, G.: Three decades of global methane sources and sinks, *Nat. Geosci.*, 6,



- 813–823, <https://doi.org/10.1038/ngeo1955>, 2013.
- 620 Kopp, R. E., DeConto, R. M., Bader, D. A., Hay, C. C., Horton, R. M., Kulp, S., Oppenheimer, M., Pollard, D. and Strauss, B. H.: Evolving Understanding of Antarctic Ice-Sheet Physics and Ambiguity in Probabilistic Sea-Level Projections, *Earth's Futur.*, 5, 1217–1233, <https://doi.org/10.1002/2017EF000663>, 2017.
- Levermann, A., Clark, P. U., Marzeion, B., Milne, G. A., Pollard, D., Radic, V. and Robinson, A.: The multimillennial sea-level commitment of global warming, *Proc. Natl. Acad. Sci. USA*, 110, 13745–13750, 625 <https://doi.org/10.1073/pnas.1219414110>, 2013.
- Levermann, A., Winkelmann, R., Albrecht, T., Goelzer, H., Golledge, N. R., Greve, R., Huybrechts, P., Jordan, J., Leguy, G., Martin, D., Morlighem, M., Pattyn, F., Pollard, D., Quiquet, A., Rodehacke, C., Seroussi, H., Sutter, J., Zhang, T., Van Breedam, J., Calov, R., DeConto, R., Dumas, C., Garbe, J., Gudmundsson, G. H., Hoffman, M. J., Humbert, A., Kleiner, T., Lipscomb, W. H., Meinshausen, M., Ng, E., Nowicki, S. M. J., Perego, M., Price, S. F., Saito, F., Schlegel, N.-J., Sun, S., and 630 van de Wal, R. S. W.: Projecting Antarctica's contribution to future sea level rise from basal ice shelf melt using linear response functions of 16 ice sheet models (LARMIP-2), *Earth Syst. Dynam.*, 11, 35–76, <https://doi.org/10.5194/esd-11-35-2020>, 2020.
- Lord, N. S., Ridgwell, A., Thorne, M. C. and Lunt, D. J.: An impulse response function for the “long tail” of excess atmospheric CO₂ in an Earth system model, *Global Biogeochem. Cycles*, 30, 2–17, <https://doi.org/10.1002/2014GB005074>, 2016.
- Loutre, M. F., Mouchet, A., Fichet, T., Goosse, H., Goelzer, H., and Huybrechts, P.: Evaluating climate model performance 635 with various parameter sets using observations over the recent past, *Clim. Past*, 7, 511–526, <https://doi.org/10.5194/cp-7-511-2011>, 2011.
- Loutre, M. F., Fichet, T., Goosse, H., Huybrechts, P., Goelzer, H., and Capron, E.: Factors controlling the last interglacial climate as simulated by LOVECLIM1.3, *Clim. Past*, 10, 1541–1565, <https://doi.org/10.5194/cp-10-1541-2014>, 2014.
- Maier-Reimer, E. and Hasselmann, K.: Transport and storage of CO₂ in the ocean - an inorganic ocean-circulation carbon 640 cycle model, *Clim. Dyn.*, 2, 63–90, <https://doi.org/10.1007/BF01054491>, 1987.
- Matthews, H.D., Zickfeld, K., Knutti, R. and Allen, M. R.: Focus on cumulative emissions, global carbon budgets and the implications for climate mitigation targets, *Environ. Res. Lett.*, 13, 010201, <https://doi.org/10.1088/1748-9326/aa98c9>, 2018.
- McGlade, C. and Ekins, P.: The geographical distribution of fossil fuels unused when limiting global warming to 2°C, *Nature*, 517, 187–190, <https://doi.org/10.1038/nature14016>, 2015.
- 645 Meinshausen, M., Smith, S. J., Calvin, K., Daniel, J. S., Kainuma, M. L. T., Lamarque, J-F., Matsumoto, K., Montzka, S. A., Raper, S. C. B., Riahi, K., Thomson, A., Velders, G. J. M. and van Vuuren, D. P. P.: The RCP greenhouse gas concentrations and their extensions from 1765 to 2300, *Clim. Change*, 109, 213–241, <https://doi.org/10.1007/s10584-011-0156-z>, 2011.
- Miller, K. G., Kominz, M. A., Browning, J. V., Wright, J. D., Mountain, G. S., Katz, M. E., Sugarman, P. J., Cramer, B. S., Christie-Blick, N. and Pekar, S. F.: The Phanerozoic Record of Global Sea-Level Change, *Science*, 310, 1293–1298, 650 <https://doi.org/10.1126/science.1116412>, 2005.
- Oppenheimer, M., Glavovic, B., Hinkel, J., van de Wal, R. S. W., Magnan, A., Abd-Elgawad, A., Cai, R., Cifuentes Jara, M., DeConto, R., Ghosh, T., Hay, J., Isla, F., Marzeion, B., Meyssignac, B., and Sebesvari, Z.: Sea Level Rise and Implications



- for Low Lying Islands, Coasts and Communities, in: IPCC Special Report on the Ocean and Cryosphere in a Changing Climate, edited by: Pörtner, H.-O., Roberts, D. C., Masson-Delmotte, V., Zhai, P., Tignor, M., Poloczanska, E., Mintenbeck, K., Nicolai, M., Okem, A., Petzold, J., Rama, B., and Weyer, N., p. 169, in press, 2019.
- 655 Opsteegh, J. D., Haarsma, R. J., Selten, F. M. and Kattenberg, A.: ECBILT: A dynamic alternative to mixed boundary conditions in ocean models, *Tellus A*, 50, 348–367, <https://doi.org/10.3402/tellusa.v50i3.14524>, 1998.
- Piñero, E., Marquardt, M., Hensen, C., Haeckel, M., and Wallmann, K.: Estimation of the global inventory of methane hydrates in marine sediments using transfer functions, *Biogeosciences*, 10, 959–975, <https://doi.org/10.5194/bg-10-959-2013>, 2013.
- 660 Pollard, D., DeConto, R. M. and Alley, R. B.: Potential Antarctic Ice Sheet retreat driven by hydrofracturing and ice cliff failure, *Earth Planet. Sci. Lett.*, 412, 112–121, <https://doi.org/10.1016/j.epsl.2014.12.035>, 2015.
- Pörtner, H.-O., Roberts, D. C., Masson-Delmotte, V., Zhai, P., Tignor, M., Poloczanska, E., Mintenbeck, K., Alegría, A., Nicolai, M., Okem, A., Petzold, J., Rama, B., and Weyer, N. W. (Eds.): IPCC Special Report on the Ocean and Cryosphere in a Changing Climate (SROCC), Cambridge University Press, in press, 2019.
- 665 Raper, S. C. B. and Braithwaite, R. J.: Low sea level rise projections from mountain glaciers and icecaps under global warming, *Nature*, 439, 311–313, <https://doi.org/10.1038/nature04448>, 2006.
- Robinson, A., Calov, R. and Ganopolski, A.: Multistability and critical thresholds of the Greenland ice sheet, *Nat. Clim. Chang.*, 2, 429–432, <https://doi.org/10.1038/nclimate1449>, 2012.
- Rogelj, J., Schaeffer, M., Friedlingstein, P., Gillett, N. P., van Vuuren, D. P., Riahi, K., Allen, M. and Knutti, R.: Differences between carbon budget estimates unravelled, *Nat. Clim. Chang.*, 6, 245–252, <https://doi.org/10.1038/nclimate2868>, 2016.
- 670 Ruppel, C. D. and Kessler, J. D.: The interaction of climate change and methane hydrates, *Rev. Geophys.*, 55, 126–168, <https://doi.org/10.1002/2016RG000534>, 2017.
- Seroussi, H., Nowicki, S., Payne, A. J., Goelzer, H., Lipscomb, W. H., Abe Ouchi, A., Agosta, C., Albrecht, T., Asay-Davis, X., Barthel, A., Calov, R., Cullather, R., Dumas, C., Gladstone, R., Golledge, N., Gregory, J. M., Greve, R., Hatterman, T., Hoffman, M. J., Humbert, A., Huybrechts, P., Jourdain, N. C., Kleiner, T., Larour, E., Leguy, G. R., Lowry, D. P., Little, C. M., Morlighem, M., Pattyn, F., Pelle, T., Price, S. F., Quiquet, A., Reese, R., Schlegel, N.-J., Shepherd, A., Simon, E., Smith, R. S., Straneo, F., Sun, S., Trusel, L. D., Van Breedam, J., van de Wal, R. S. W., Winkelmann, R., Zhao, C., Zhang, T., and Zwinger, T.: ISMIP6 Antarctica: a multi-model ensemble of the Antarctic ice sheet evolution over the 21st century, *The Cryosphere Discuss.*, <https://doi.org/10.5194/tc-2019-324>, in review, 2020.
- 680 Solomon, S., Plattner, G. K., Knutti, R. and Friedlingstein, P.: Irreversible climate change due to carbon dioxide emissions, *Proc. Natl. Acad. Sci. USA*, 106, 1704–1709, <https://doi.org/10.1073/pnas.0812721106>, 2009.
- Swingedouw, D., Fichfet, T., Huybrechts, P., Goosse, H., Driesschaert, E. and Loutre, M. F.: Antarctic ice-sheet melting provides negative feedbacks on future climate warming, *Geophys. Res. Lett.*, 35, 2–5, <https://doi.org/10.1029/2008GL034410>, 2008.
- 685 Treude, T., Boetius, A., Knittel, K., Wallmann, K. and Jørgensen, B. B.: Anaerobic oxidation of methane above gas hydrates at Hydrate Ridge, NE Pacific Ocean, *Mar. Ecol. Prog. Ser.*, 264, 1–14, <https://doi.org/10.3354/meps264001>, 2003.



- Vizcaíno, M., Mikolajewicz, U., Gröger, M., Maier-Reimer, E., Schurgers, G. and Winguth, A. M. E.: Long-term ice sheet-climate interactions under anthropogenic greenhouse forcing simulated with a complex Earth System Model, *Clim. Dyn.*, 31, 665–690, <https://doi.org/10.1007/s00382-008-0369-7>, 2008.
- 690 Watson, C. S., White, N. J., Church, J. A., King, M. A., Burgette, R. J. and Legresy, B.: Unabated global mean sea-level rise over the satellite altimeter era, *Nat. Clim. Chang.*, 5, 565–568, <https://doi.org/10.1038/nclimate2635>, 2015.
- WCRP Global Sea Level Budget Group: Global sea-level budget 1993–present, *Earth Syst. Sci. Data*, 10, 1551–1590, <https://doi.org/10.5194/essd-10-1551-2018>, 2018.
- Winkelmann, R., Levermann, A., Martin, M. A. and Frieler, K.: Increased future ice discharge from Antarctica owing to higher
695 snowfall, *Nature*, 492, 239–242, <https://doi.org/10.1038/nature11616>, 2012.
- Winkelmann, R., Levermann, A., Ridgwell, A. and Caldeira, K.: Combustion of available fossil fuel resources sufficient to eliminate the Antarctic Ice Sheet, *Sci. Adv.*, 1, 1–6, <https://doi.org/10.1126/sciadv.1500589>, 2015.
- Zeebe, R. E. and Zachos, J. C.: Long-term legacy of massive carbon input to the Earth system: Anthropocene versus Eocene, *Phil. Trans. R. Soc. A*, 371, 20120006, <https://doi.org/10.1098/rsta.2012.0006>, 2013.
- 700 Zickfeld, K., Arora, V. K. and Gillett, N. P.: Is the climate response to CO₂ emissions path dependent?, *Geophys. Res. Lett.*, 39, 1–6, <https://doi.org/10.1029/2011GL050205>, 2012.

705

710

715



720 **Table 1: Sea-level contribution from the different components contributing to GMSL change for scenario MMCP2.6, MMCP4.5, MMCP6.0, MMCP-break, MMCP8.5 and MMCP-feedback shown in meters and as a percentage of GMSL change.**

	Antarctic ice sheet	Greenland ice sheet	Steric component	Glaciers and ice caps	GMSL rise
MMCP2.6	1.6 m (17.4 %)	7.0 m (76.1 %)	0.4 m (4.3 %)	0.23 m (2.5 %)	9.2 m
MMCP4.5	1.9 m (18.8 %)	7.3 m (72.3 %)	0.7 m (6.9 %)	0.23 m (2.3 %)	10.1 m
MMCP6.0	6.6 m (42.9 %)	7.3 m (47.4 %)	1.3 m (8.4 %)	0.24 m (1.6 %)	15.4 m
MMCP-break	12.0 m (54.8 %)	7.4 m (33.8 %)	2.3 m (10.5 %)	0.24 m (1.1 %)	21.9 m
MMCP8.5	19.7 m (65.4 %)	7.4 m (24.6 %)	2.8 m (9.3 %)	0.24 m (0.8 %)	30.1 m
MMCP-feedback	26.8 m (71.7 %)	7.4 m (19.8 %)	3.0 m (8.0 %)	0.24 m (0.6 %)	37.4 m

Table A1: Estimates of CO₂ airborne fractions available in the literature 1000 and 10,000 years after a pulse of CO₂ into the atmosphere.

Reference	CO ₂ emission pulse (GtC)	AF (1000 year)	AF (10,000 year)
(Archer and Brovkin, 2008)	1000	29 %	14 %
	5000	57 %	26 %
(Archer et al., 2009a)	1000	24-31 %	10-21 %
	5000	32-62 %	14-32 %
(Eby et al., 2009)	1000	30 %	17 %
	5000	60 %	30 %
(Joos et al., 2013)	100	10-21 %	/
	100 (+350)	20-30 %	/
	5000	30-60 %	/

725

730

735



740

Table A2: Average equilibrium airborne fractions for total emissions of around 500 to 5000 GtC according to the values given in Table A1. The equilibrium airborne fraction for 2000 GtC is extrapolated from the average equilibrium airborne fraction for the 1000 GtC and 5000 GtC scenarios. The instantaneous airborne fraction is the airborne fraction reached after one year (AF^{peak}). Airborne fractions after 1000 and 10,000 years are given. The columns highlighted in bold give the fractions of atmospheric CO_2 still present 1000 and 10,000 years after the peak concentration. The numbers in the first column denote the cumulative emissions CO_2 emissions with respect to pre-industrial.

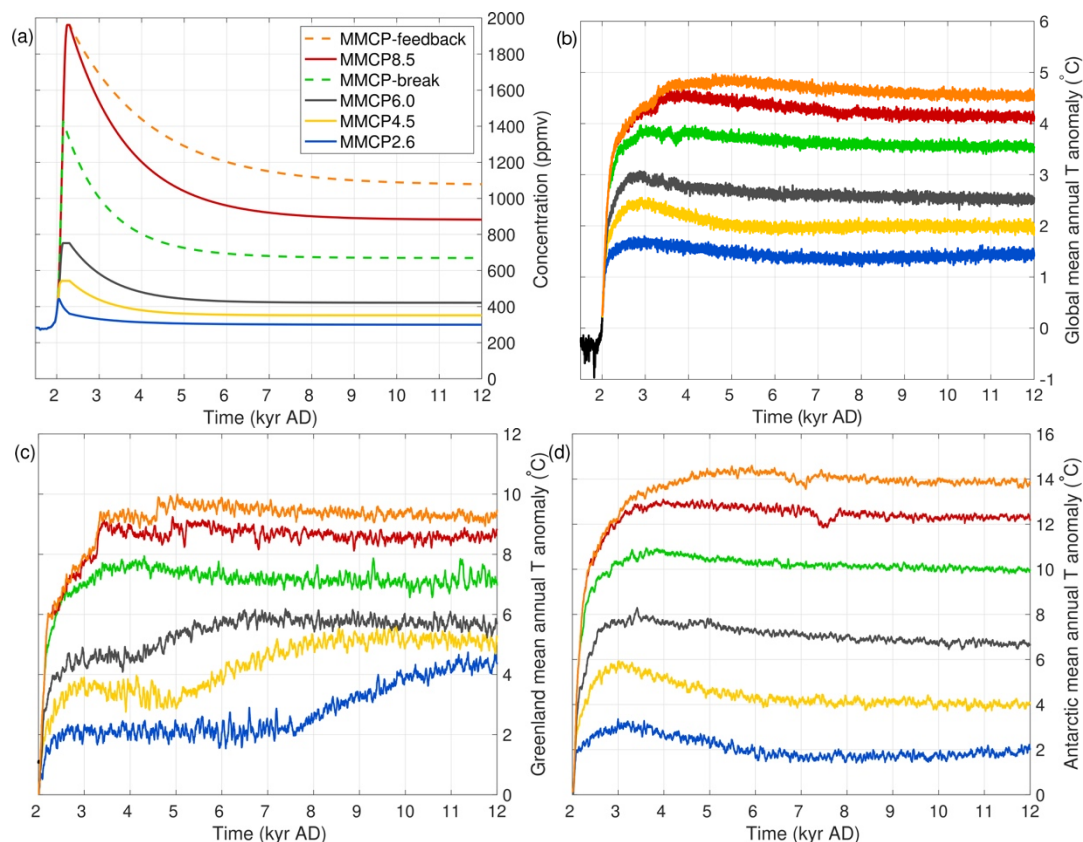
	AF^{peak}	AF_s^{equi} (1000 years)	$\frac{AF_s^{\text{equi}}}{AF^{\text{peak}}}$	AF_l^{equi} (10,000 years)	$\frac{AF_l^{\text{equi}}}{AF^{\text{peak}}}$
461 GtC – MMCP2.6 (low)	50 %	25 %	50 %	12 %	24 %
1361 GtC – MMCP4.5 (moderate)	55 %	28 %	51 %	15 %	27 %
2234 GtC – MMCP6.0 (moderate)	60 %	33 %	55 %	18 %	30 %
3393 GtC – MMCP-break (high)	65 %	40 %	62 %	22 %	34 %
5288 GtC – MMCP8.5 (high)	70 %	47 %	67 %	25 %	36 %
5888 GtC – MMCP-feedback (high)	70 %	55 %	78 %	33 %	47 %

745

Table A3: Different CO_2 scenarios used in the simulations with their time of peak concentration, the values for the peak concentration, the mean concentration over the next 10,000 years and the equivalent total emissions (calculated as in Meinshausen et al. (2011)). The total cumulative emissions are an approximation for the RCP scenarios (the numbers give the total fossil fuel cumulative CO_2 emissions expressed in GtC for the period 2000-2300 AD). These numbers are on top of the cumulative CO_2 emissions before 2000 AD given in brackets (about 270 GtC; Ciais et al. (2013)).

Scenario	Time of peak concentration	Peak concentration (ppmv)	Mean concentration (ppmv)	Cumulative emissions (GtC)
MMCP2.6	2053	443	305	191 (+270)
MMCP4.5	2130	543	358	1091 (+270)
MMCP6.0	2150	752	431	1964 (+270)
MMCP-break	2150	1429	674	3723 (+270)
MMCP8.5	2250	1962	918	5018 (+270)
MMCP-feedback	2250	1962	1088	5618 (+270)

750

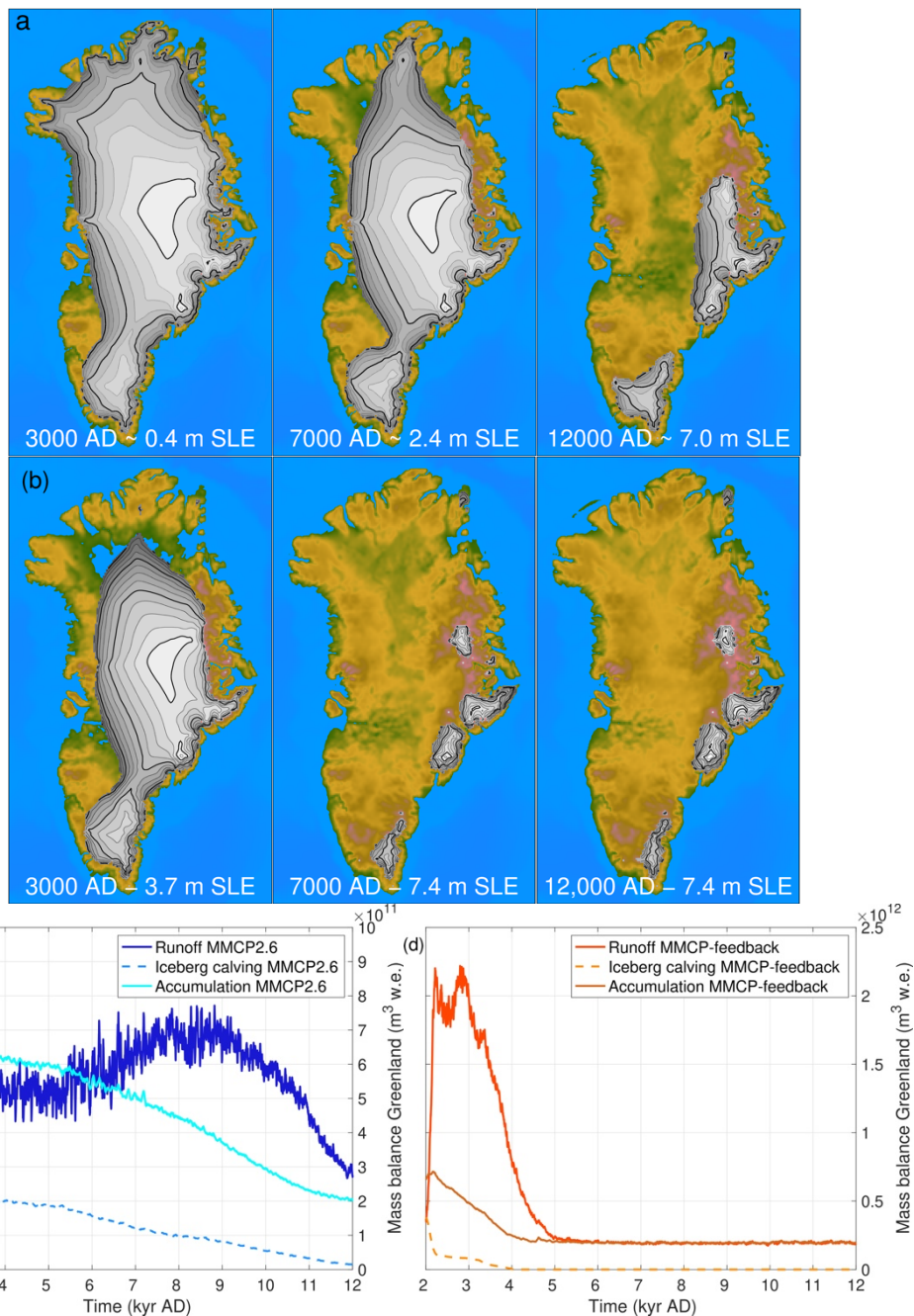


755 **Figure 1: (a) Atmospheric CO₂ concentration scenario from 1500 AD to 12,000 AD for the six different forcing scenarios. The four RCP-based scenarios are given in solid lines, while the two additional scenarios are shown as dashed lines. (b) Global mean temperature change for the historical period 1500-2000 AD and the future projections (c) Greenland mean temperature change and (d) Antarctic mean temperature change for the six forcing scenarios. All temperature projections are shown as an anomaly to a reference period 1970-2000.**

760

765

770

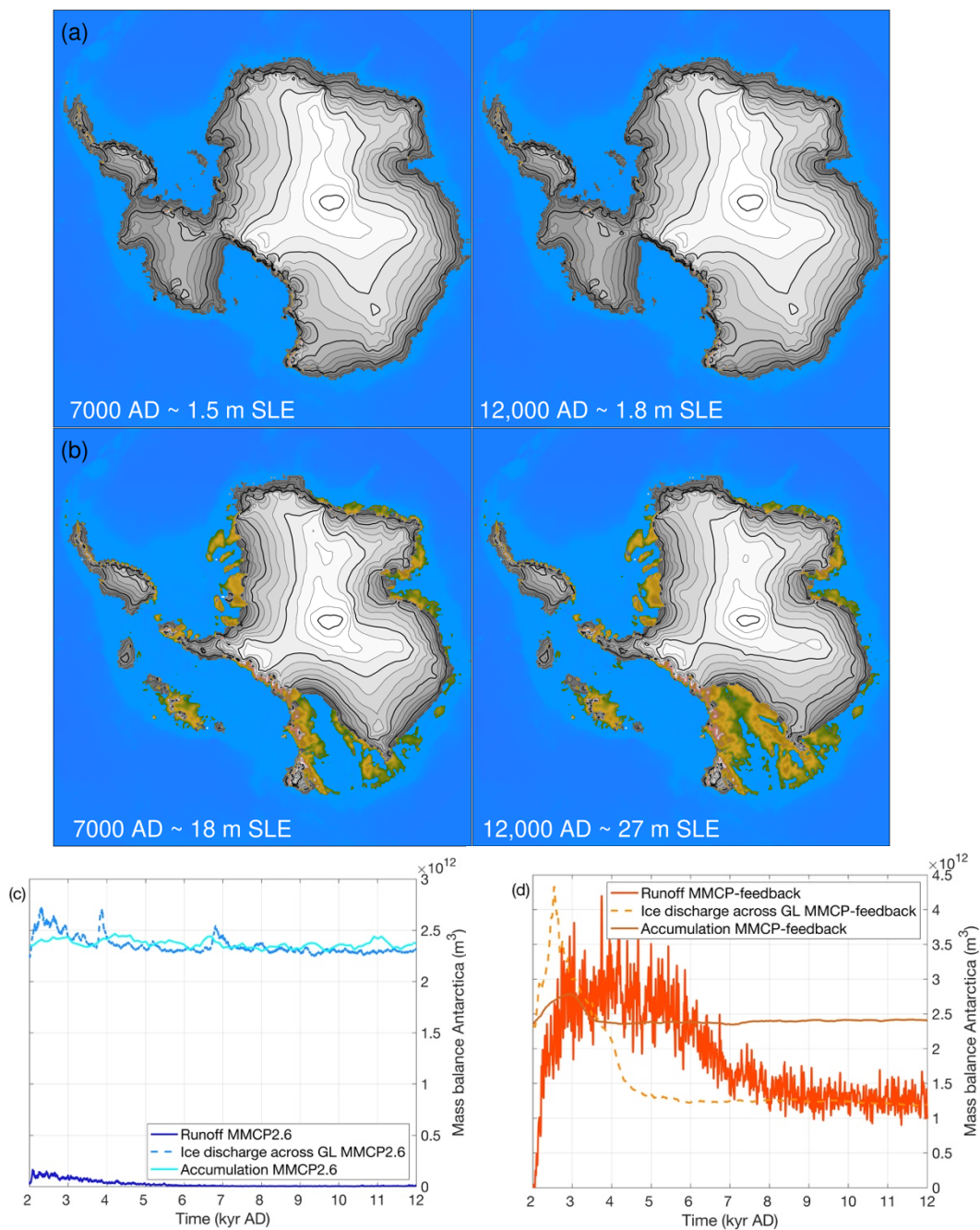


775

Figure 2: (a) Greenland ice sheet configuration at 3,000 AD, 7,000 AD and 12,000 AD using scenario MMCP2.6 and (b) MMCP-feedback. Main mass balance components explaining the change in ice sheet geometry for scenarios MMCP2.6 (c) and MMCP-feedback (d).

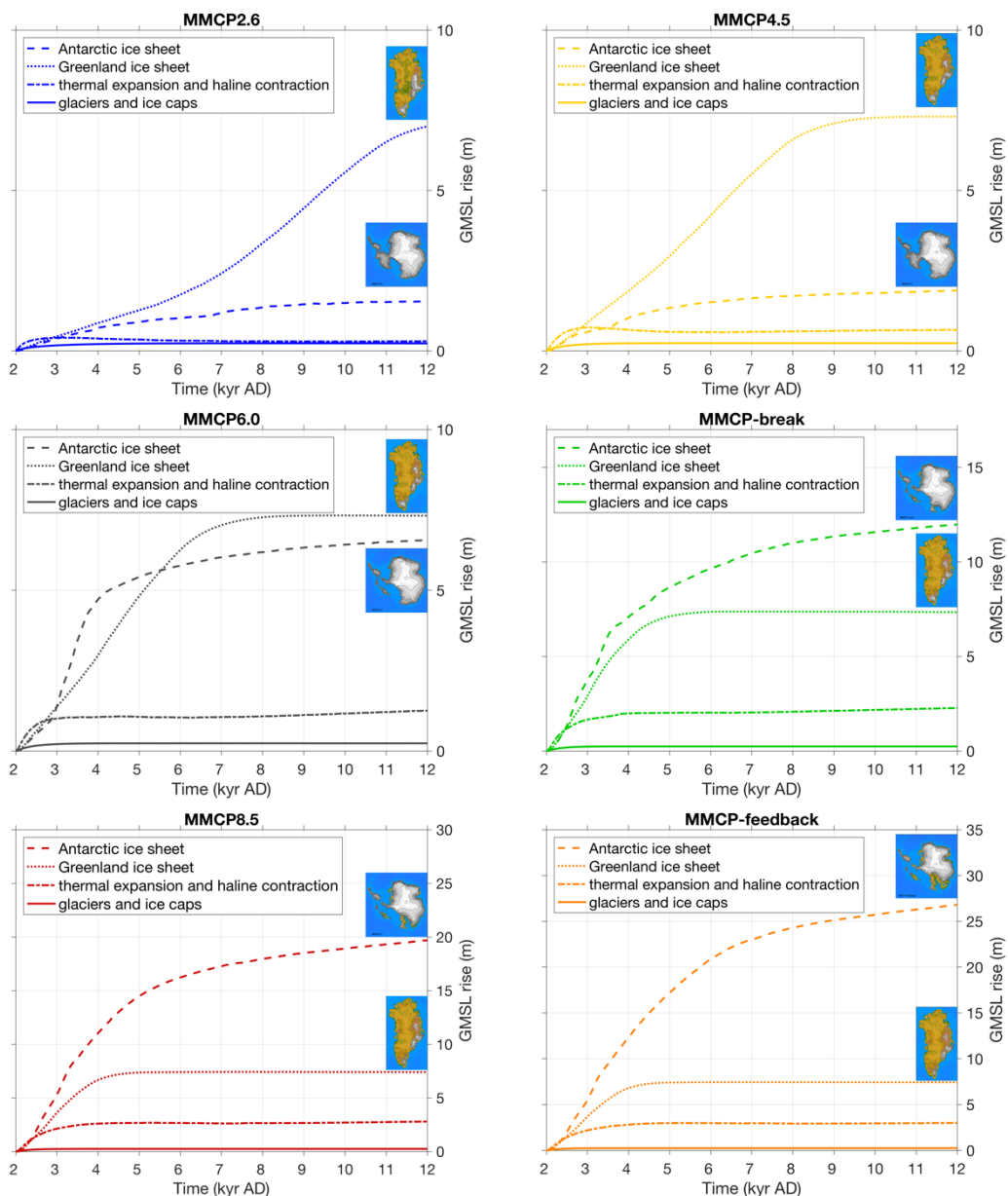


780



785

Figure 3: (a) Antarctic ice sheet configuration at 7000 AD and 12000 AD using scenario MMCP2.6 and (b) MMCP-feedback. Main mass balance components (over grounded ice) explaining the change in ice sheet geometry for scenarios MMCP2.6 (c) and MMCP-feedback (d). GL=grounding line.



790

Figure 4: The contribution of the different components to GMSL rise during the next 10,000 years for each of the forcing scenarios. The ice sheet geometry of Greenland and Antarctica is shown at the end of the simulations.

795

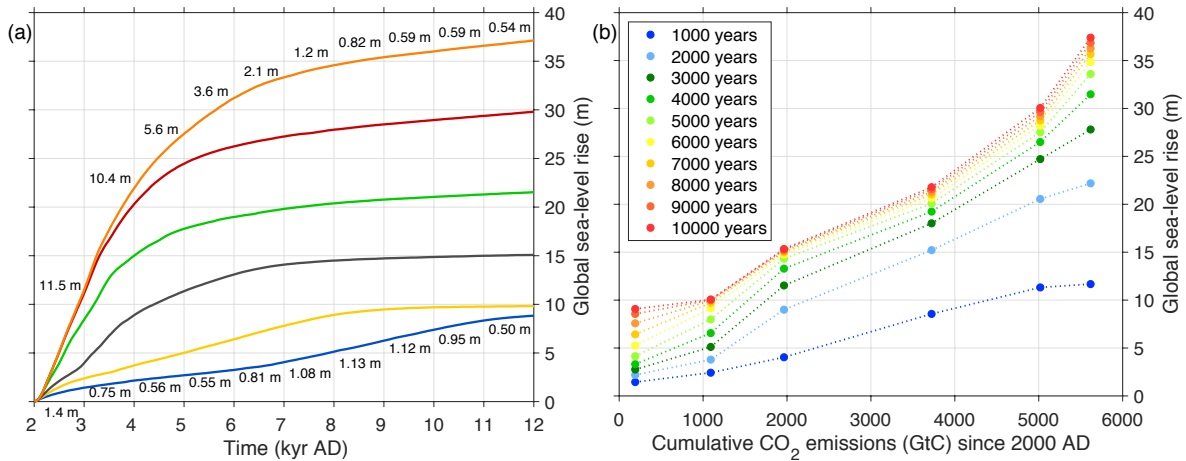
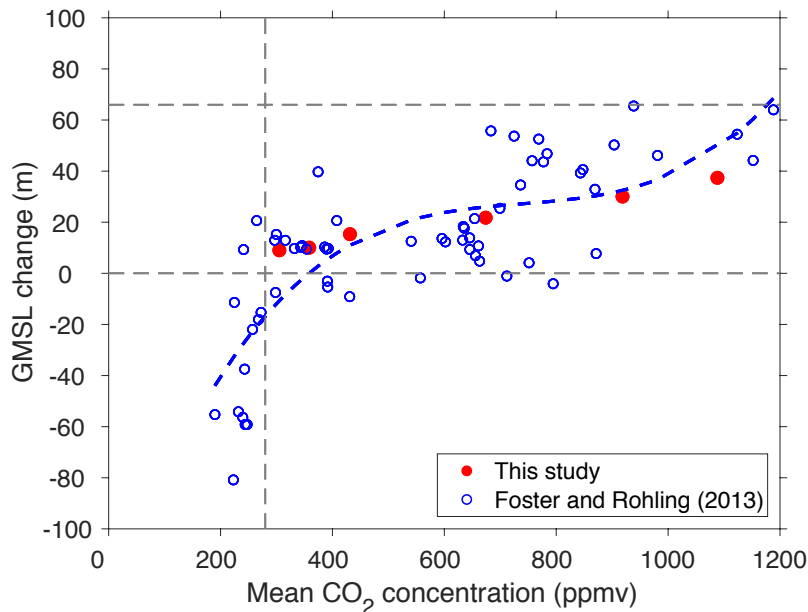


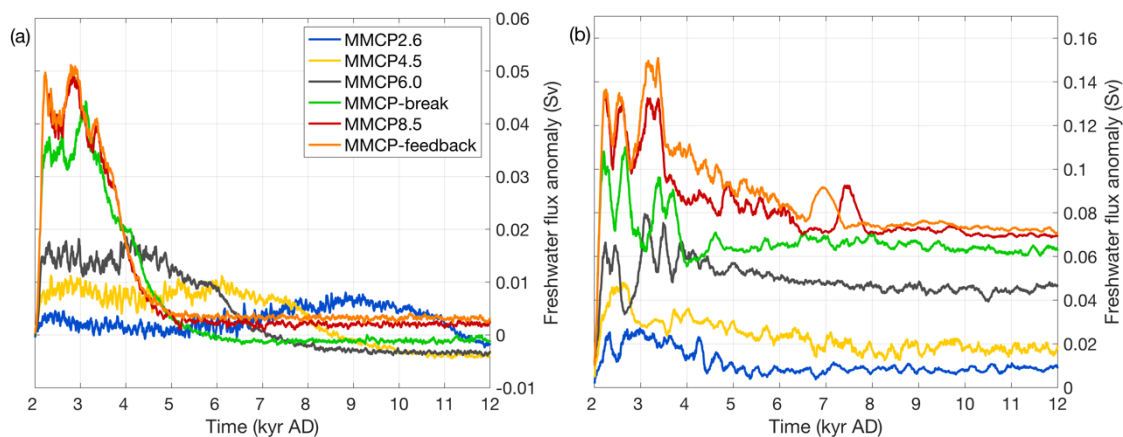
Figure 5: (a) GMSL rise as the sum of the contributions from the AIS, the GrIS, glaciers and ice caps, and thermal expansion and haline contraction. The rate of sea level rise during each millennium is indicated for the lowest and highest scenarios. (b) GMSL rise for a given cumulative CO₂ emission at the end of each millennium until 12,000 AD.

800

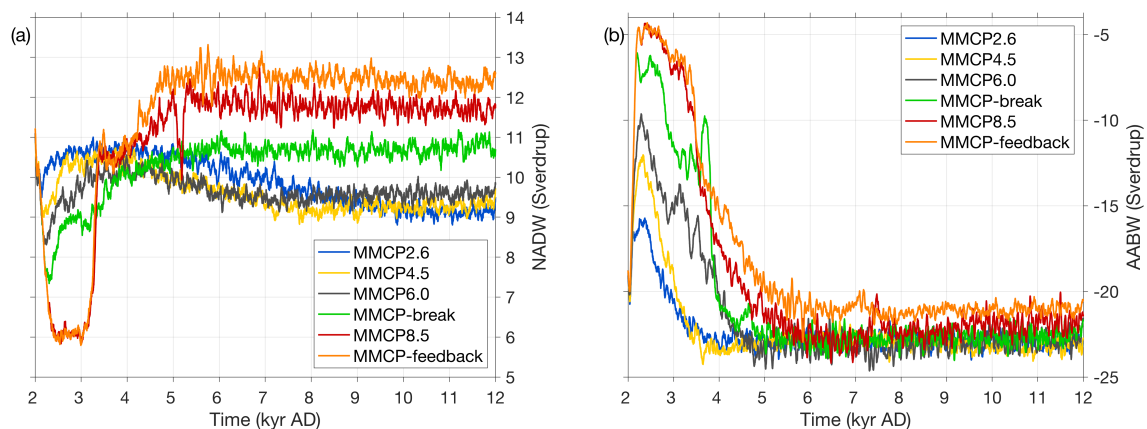


805

Figure 6: Semi-equilibrated GMSL change projections at 12,000 AD compared to the geological record of sea-level high stands (Foster and Rohling, 2013) for a given atmospheric CO₂ concentration. The atmospheric CO₂ concentrations used for the projections of GMSL are averaged over the 10,000-year simulation. The horizontal line at 0 m GMSL change represents the present-day situation and the horizontal line at +65 m is equivalent to melting all land ice on Earth.



810 **Figure 7: Freshwater flux anomalies with respect to 1970–2000 from the Greenland ice sheet (a) and the Antarctic ice sheet (b) for the six different forcing scenarios.**



815 **Figure 8: Mean annual strength of the North Atlantic Deepwater (NADW) (a) and the Antarctic Bottom Water (AABW) (b) formation from 2000 AD to 12,000 AD. AABW is defined as the maximum of the global meridional overturning streamfunction in the bottom cell and NADW as the maximum of the meridional overturning circulation in the Greenland, Iceland and Norwegian Seas.**

820

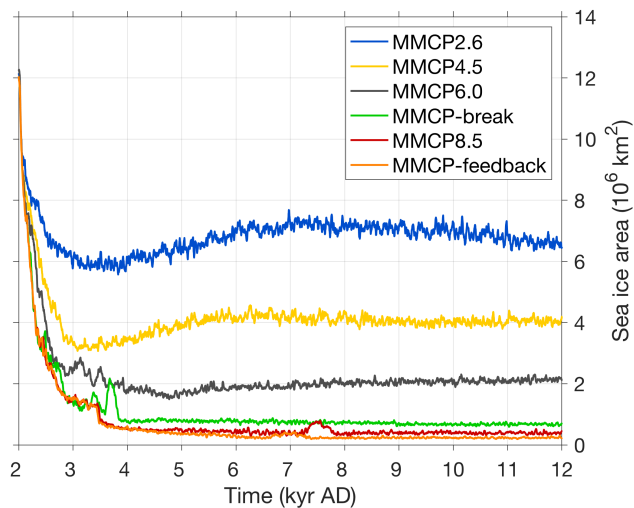
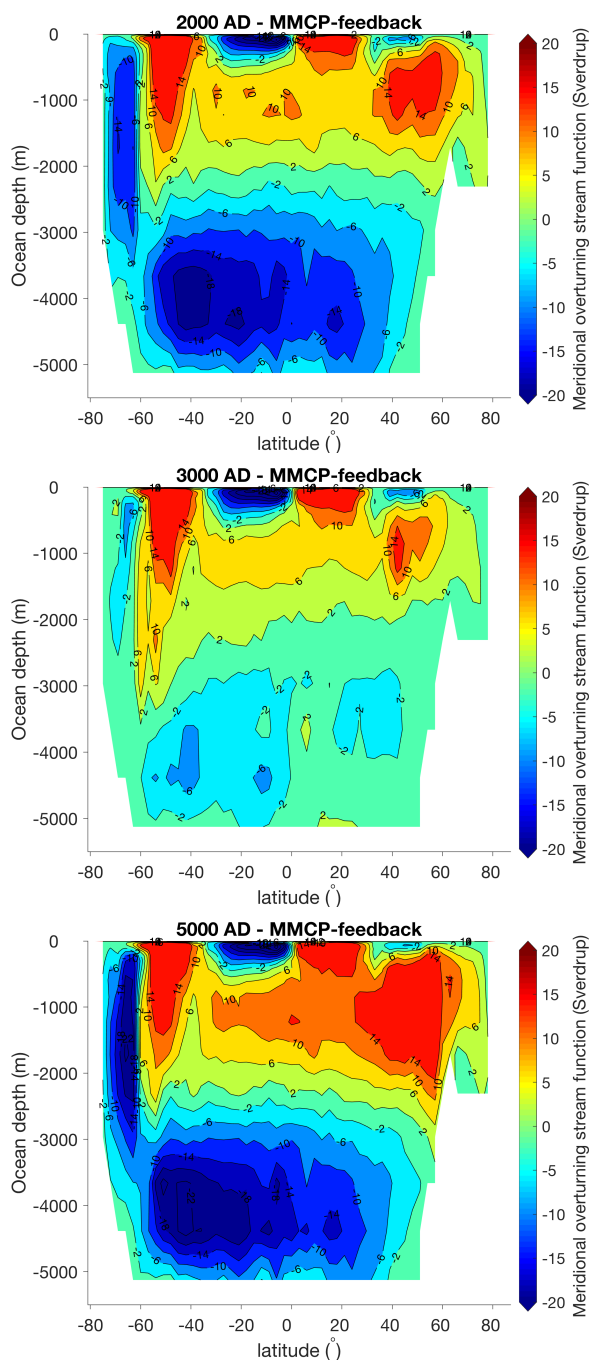


Figure 9: Mean sea-ice area evolution in the Southern Ocean for the six different forcing scenarios.

825

830

835

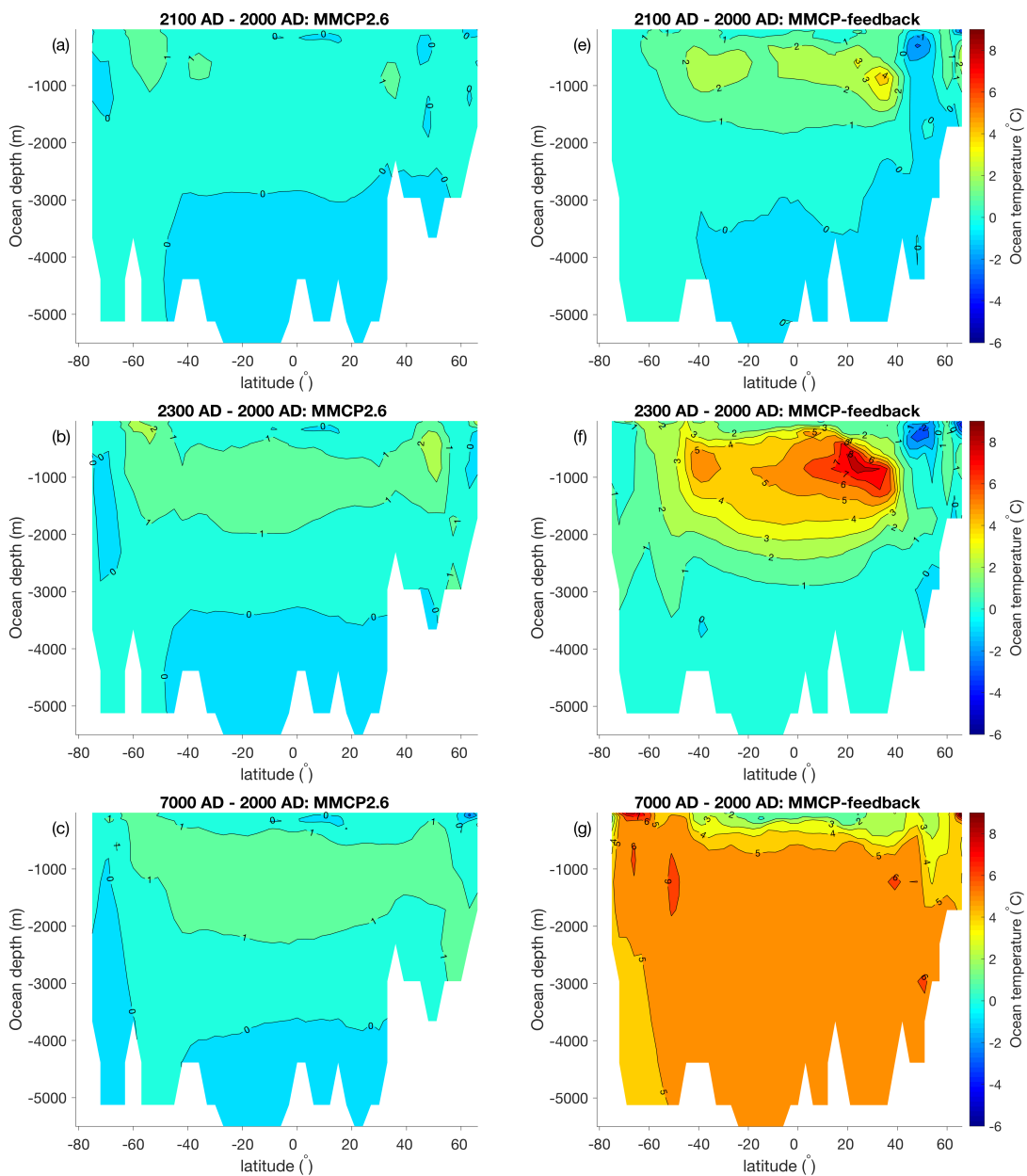


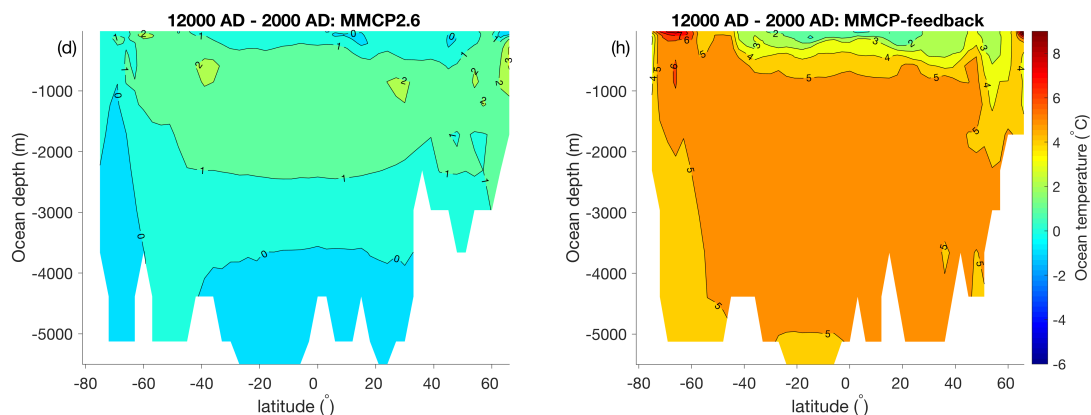
840

Figure 10: Meridional overturning stream function for the global ocean at 2000 AD, 3000 AD and 5000 AD using forcing scenario MMCP-feedback.



845





850 **Figure 11: Ocean temperature anomaly across the Atlantic ocean using scenario MMCP2.6 at 2100 AD (a), 2300 AD (b), 7000 AD (c), 12,000 AD (d) and using scenario MMCP-feedback at 2100 AD (e), 2300 AD (f), 7000 AD (g), 12,000 AD (h).**

855